

See discussions, stats, and author profiles for this publication at: <https://www.researchgate.net/publication/8633482>

Can One Assess the π Character of a C–C Bond with the Help of the NMR Spin–Spin Coupling Constants?

ARTICLE *in* CHEMPHYSCHEM · MARCH 2004

Impact Factor: 3.42 · DOI: 10.1002/cphc.200300987 · Source: PubMed

CITATIONS

25

READS

25

4 AUTHORS, INCLUDING:



[Elfi Kraka](#)

Southern Methodist University

168 PUBLICATIONS **5,678** CITATIONS

SEE PROFILE



[Anan Wu](#)

Xiamen University

41 PUBLICATIONS **761** CITATIONS

SEE PROFILE

Can One Assess the π Character of a C–C Bond with the Help of the NMR Spin–Spin Coupling Constants?

Dieter Cremer,^{*,[a]} Elfi Kraka,^[a] Anan Wu,^[a] and Wolfgang Lüttke^[b]

Measured one-bond spin–spin coupling constants (SSCC) $^1J(\text{CC})$ can be used to describe the nature of the C–C bond, provided one is able to separate the various coupling mechanisms leading to $^1J(\text{CC})$. The Fermi-contact (FC) term probes the first-order density at the positions of the coupling nuclei, whereas the noncontact terms (the paramagnetic spin orbit (PSO) and the spin–dipole (SD) terms) probe the π character of the C–C bond (the diamagnetic spin orbit (DSO) term can mostly be neglected). A model is tested, in which the value of the FC(CC) term is estimated with the help of measured SSCCs $^1J(\text{CH})$. The difference between the measured $J(\text{CC})$

and the estimated FC(CC) values, $\Delta(\text{CC}) = \text{PSO}(\text{CC}) + \text{SD}(\text{CC}) + \text{DSO}(\text{CC})$, provides a semiquantitative measure of the π character of a C–C multiple bond. The applicability and limitations of this approach are discussed by partitioning the four Ramsey terms of the SSCC $^1J(\text{CC})$ into one- and two-orbital contributions. The FC, PSO, and SD terms of $^1J(\text{CC})$ are explained and analyzed with regard to their relationship to other C–C bond properties. It is shown that empirical relationships between measured SSCCs and the s character of a bond need reconsideration.

1. Introduction

One of the most successful concepts in chemistry is the concept of the chemical bond.^[1–8] The chemical bond is not an observable quantity in so far as there are no bond properties which can be measured.^[8] Nevertheless, one tries to assess the nature of the chemical bond from measured properties, such as the bond dissociation energy, the bond length, the bond stretching frequency, the bond dipole moment, and so on. It is easy to see that each of these properties can only provide a limited insight into the nature of the chemical bond, because they also depend on things other than bond properties, or they cannot be directly measured.^[7–10] For example, the bond dissociation energy also depends on the (de)stabilization of the bond fragments and therefore cannot be used as a direct measure of the bond strength.^[9–11] The bond length is actually just the direct distance between bonded atoms, but the bond can be curved, thus leading to a larger bond length than given by this distance.^[12] The bond-stretching force constant cannot directly be measured.^[10] It can only be derived within a suitable model of the bond and its dynamic behavior within the molecule.^[9, 10] The same applies to the bond dipole moment, which must be derived from the total molecular dipole moment and appropriate atomic charges, using a particular model.^[10]

Since the experimentally based bond properties, such as bond length, bond dissociation energy, and so on, have their deficiencies, it is of general interest to define bond properties that are easy to measure and typical of a given bond. The NMR spin–spin coupling constant (SSCC) $^1J(\text{A,B})$ could be such a property, and there have been—in particular for hydrocarbons—many attempts to relate $^1J(\text{C,H})$ and $^1J(\text{CC})$ to other bond

properties, such as the s character of the localized molecular orbitals (LMOs) describing the C–H or C–C bond, the $\pi(\text{CC})$ bond order in benzenoid compounds, or the C–C bond length.^[13–22] In particular, simple models relating the s character of hybrid orbitals to both the bond strength and the SSCC $^1J(\text{C,H})$ or $^1J(\text{CC})$ have been very successful and have supported the idea that the SSCC is a suitable molecular parameter for describing the nature of the chemical bond. Possible extensions of the relationships found for C–H and C–C bonds have been investigated and found for other bonds, such as C–N, N–H, and so on.^[23]

In this Article, we investigate whether the SSCC $^1J(\text{A,B})$ is a suitable molecular property for describing the nature of the chemical bond.^[24] For this purpose, we will consider the spin–spin coupling mechanism in detail, using orbital theory.^[25] There are four different contributions (Ramsey terms),^[26] which probe different parts of the electron density, either more the σ or more the π density. If it is possible to separate the various terms of measured one-bond SSCC $^1J(\text{A,B})$, then it should be possible to determine the nature of a bond. We will develop such an approach for one-bond $^{13}\text{C}^{13}\text{C}$ coupling constants (henceforth called $^1J(\text{CC})$) and investigate its usefulness. The reason for

[a] Professor D. Cremer, Professor E. Kraka, Dr. A. Wu
Department of Theoretical Chemistry, Göteborg University
Reutersgatan 2, S-413 20 Göteborg (Sweden)
E-mail: Dieter.Cremer@Theoc.gu.se

[b] Professor W. Lüttke
Institut für Organische Chemie, Universität Göttingen
Tammanstr. 2, Göttingen (Germany)

choosing $^1J(\text{CC})$ constants is two-fold: There are many experimental $^1J(\text{CC})$ ^[19] and associated $^1J(\text{C,H})$ values,^[20] so that unusual C–C bonding situations can also be documented by the SSCCs. Secondly, the one-bond spin–spin coupling mechanism is easier to describe when the bond in question does not include a heteroatom. The lone-pair electrons of the latter make a large contribution to the coupling mechanism,^[25] thus complicating the relationship between bond properties and the SSCC.

Focusing exclusively on C–C coupling, the one-bond SSCCs will be investigated with the help of additional quantum chemical calculations. We will discuss the Ramsey terms of the SSCC by decomposing them into orbital contributions. In this respect, we will show that not only the C–C bond orbital and its associated density, but also the bond orbitals involved in substituent bonding, play an important role in the one-bond coupling constant. We will present results by first discussing a suitable way of partitioning measured $^1J(\text{CC})$ values into Ramsey terms (Section 2). Then we will describe the basis of a quantum chemical analysis of the different coupling terms (Section 3), and then present a detailed analysis of C–C spin–spin coupling for different bonding situations (Section 4). Finally, we will discuss the chemical relevance of our results.

2. The σ/π Character of a C–C Bond and the Spin–Spin Coupling Constant

According to the theory of Ramsey,^[26] the indirect isotropic SSCC can be understood in the way that one of the nuclei (called the *perturbing nucleus* in the following) perturbs, by its magnetic moment, the electron system, which in turn gives rise to a magnetic field at the location of the second (*responding*) nucleus. There are four different spin–spin coupling mechanisms contributing to the isotropic SSCC: The Fermi-contact (FC) term is a response property that reflects the interaction between the spin magnetic moment of the electrons at the contact surface of the nucleus and the magnetic field inside the nucleus. This leads to spin polarization at the contact surface, which travels through the molecule and causes spin polarization at the contact surface of other nuclei, which in turn determines, by Fermi coupling, the orientation of the nuclear spin magnetic moment. The FC term probes the spin polarization of the s electrons only, because electrons with higher angular momentum have a zero probability of being found at the nuclear contact surface. In the case of the spin–dipole (SD) term, it is the magnetic field of the nuclear moment outside the nucleus that causes spin polarization of the molecular density and by this a coupling to the dipole fields of other nuclei, that is, the interaction between the nuclear magnetic moments is mediated by the spin angular momentums of the electrons. Analysis of the SD term shows that, in the case of C–C bonding, only the $p\pi$ electrons can contribute to this coupling mechanism.

The diamagnetic spin–orbit (DSO) and the paramagnetic spin–orbit (PSO) terms represent the interactions of the magnetic field of the nuclei transmitted by the orbital motion of the electrons. The perturbing nucleus induces a current density in the electron system, which in turn gives rise to an extra magnetic field. The value and orientation of this field at the

responding nucleus favors either a parallel or an antiparallel orientation of the perturbing and responding nuclei. The DSO and PSO terms, although they cannot be strictly separated, describe different induction mechanisms. The DSO term describes the induction of ring currents by Larmor precession, which is present for any orbital. The PSO term, in contrast, describes the modification of existing ring currents by the magnetic moment. Since the PSO operator is an angular momentum operator, the changes in the orbital currents involve $p\sigma$ and $p\pi$ electrons. Thus, the PSO term probes all p electrons, whereas the SD term depends only on the π electrons, in the case of C–C bonding. It is noteworthy that the diamagnetic and paramagnetic terms are related to similar terms, which contribute to the NMR shielding constant.^[19, 20]

For an accurate quantum chemical description of SSCCs, all four terms have to be considered,^[26–28] as shown in Equation (1)

$$^nJ(\text{A,B}) = {}^n\text{FC}(\text{A,B}) + {}^n\text{PSO}(\text{A,B}) + {}^n\text{DSO}(\text{A,B}) + {}^n\text{SD}(\text{A,B}) \quad (1)$$

where n is the number of bonds connecting the coupling nuclei A and B (in the following, $n=1$ and $\text{A}=\text{B}=\text{carbon}$, is considered).

In Table 1, the calculated SSCCs $^1J(\text{CC})$ and the Ramsey terms are listed for ethane, ethene, and acetylene. In all three cases, the FC term dominates the value of the SSCC. The NC (noncontact) terms PSO, DSO, and SD make only a small contribution in the case of the CC bond in ethane, as they do for most CC single

Table 1. Calculated NMR spin–spin coupling constants $^1J(\text{CC})$ and their Ramsey terms for ethane, ethene, and acetylene.^[a]

Molecule	$^1J(\text{CC})$	FC(CC)	PSO(CC)	SD(CC)	DSO(CC)	Δ
ethane	33.74	32.50	0.02	1.08	0.14	1.24
ethene	70.62	76.88	–10.28	3.94	0.08	–6.26
acetylene	201.73	181.67	8.38	11.60	0.08	20.06

[a] All SSCC in Hz. CP-DFT/B3LYP[7s,6p,2d/4s,2p] calculations. Δ is the sum of the noncontact terms.

bonds. With decreasing multiple bond character of the CC bond, both the PSO and SD terms increase in magnitude, namely from 0 to $|-10.3|$ and 8.4 Hz, and from 1.1 to 3.9 and 11.6 Hz, respectively (Table 1). The sum of the NC terms (1.2, –6.3, 20.06 Hz) reflects the increasing π character of the C–C bond in ethane, ethene, and acetylene, where the different signs for the PSO term of ethene and acetylene have to be considered. These trends are reproduced by all SSCC calculations.

Considering the fact that the FC term depends on the s electrons, and by this indirectly on the σ -electron distribution in a hydrocarbon, and that the NC terms PSO, DSO, and SD are either small or depend on the π -electron distribution, it should be possible to separate the FC and NC contributions to the SSCC within a suitable model and in this way to assess the π character of a bond. This might be of particular advantage in those cases where simple $\sigma-\pi$ separation models do not function because

of the nonplanarity of the molecular framework, or because of the existence of bent bonds, as in strained ring systems.^[8, 12]

Therefore, we discuss the following procedure for hydrocarbons for separating the FC and NC terms in measured $^1J(\text{CC})$ values.^[24] For a molecule such as ethene, the SSCCs $^1J(\text{CC})$ and $^1J(\text{C,H})$ are known.^[19] The former is used to assess the s character of the hybrid orbital forming the C–H bond according to the relationship described by Equation (2a).^[13, 14]

$$^1J(\text{C,H}) = a_{\text{CH}} s_{\text{C}} s_{\text{H}} - b_{\text{CH}} \quad (2a)$$

By assuming that the s character s_{H} is equal to 1 and that the constant b_{CH} is equal to zero, the Muller–Pritchard relationship, Equation 2b, was derived for the measured $^1J(\text{C,H})$ values of ethane, ethene, and acetylene.^[13]

$$^1J(\text{C,H}) = 500 s_{\text{C}} \quad (2b)$$

On the basis of SSCC calculations, slightly different Equations (2b) with a finite value for constant b_{CH} were obtained.^[14, 18, 19] If the hybrid orbital is given by $h = N(2s + \lambda \times 2p)$ —where N is the normalization constant—the mixing parameter λ will determine the s (or p) character of the orbital according to Equations (3a) and (3b).^[18]

$$\lambda^2 = \frac{(1-s)}{s} \quad (3a)$$

$$s = \frac{1}{1 + \lambda^2} \quad (3b)$$

Equation (2a) will be only valid if the NC terms do not contribute to $^1J(\text{C,H})$ significantly, so that $^1J(\text{C,H}) \approx ^1\text{FC}(\text{C,H})$, which is indeed fulfilled for most CH bonds. However, a caveat is appropriate with regard to the assumption that the s character at the H nucleus is constant. This will only be fulfilled if the C–H bond polarity does not change. One has, however, to consider that an sp -hybridized carbon atom is more electronegative than an sp^2 -hybridized carbon atom, which in turn is more electronegative than a sp^3 -hybridized carbon atom. This corresponds to

a change in the C–H bond polarity and a change in the s density at the hydrogen atom. (In quantum chemical calculations, an admixture of p -type polarization functions at the hydrogen atom becomes necessary).

Once the s character of all hybrid orbitals forming C–H bonds is known (all $^1J(\text{CH})$ values are measured), it is possible to derive the s character of the two hybrid orbitals forming the C–C bond by utilizing the sum rule for hybrid orbitals.^[18] The s character for C_{A} and C_{B} are in turn related to the FC term of $^1J(\text{CC})$ by Equation (4),^[16, 19] derived for standard C–C single bonds.

$$^1\text{FC}(\text{CC}) = a_{\text{CC}} s_{\text{A}} s_{\text{B}} - b_{\text{CC}} \quad (4)$$

By subtracting the calculated value $^1\text{FC}(\text{CC})$ from the measured value $^1J(\text{CC})$, using Equation (5), a reasonable estimate of the NC terms was obtained.

$$\Delta = ^1J(\text{CC}) - ^1\text{FC}(\text{CC}) = ^1\text{PSO}(\text{CC}) + ^1\text{DSO}(\text{CC}) + ^1\text{SD}(\text{CC}) \approx ^1\text{PSO}(\text{CC}) + ^1\text{SD}(\text{CC}) \quad (5)$$

It is safe to neglect the DSO term because of its small magnitude. Since the PSO and the SD term both depend on the π character of the bond, Equation (5) should provide a measure of the multiple bond character of the C–C bond investigated.

In the case of ethene, values of $^1J(\text{C,H}) = 156.15$ and $^1J(\text{CC}) = 67.75$ Hz have been measured.^[19] The s character of the hybrid orbital forming the C–H bond is defined by Equation (2b) to be 0.312, which leads, according to the sum rule, to an s character of $1 - (2 \times 0.312) = 0.375$ for the hybrid orbitals forming the C–C σ bond. By using 658 and -7.9 Hz^[22] (other possibilities are 576 and -3.4 ,^[16] 637 and -11 Hz^[19]) for a_{CC} and b_{CC} in Equation (4), one obtains $^1\text{FC}(\text{CC}) = 658 \times 0.375^2 - 7.9 = 84.63$ Hz. The difference—Equation (5)—is then -17.03 Hz (-14.97 Hz or -16.62 Hz). These values show that the estimated NC contribution is definitely negative, however, it varies considerably, depending on the parameters a_{CC} and b_{CC} chosen for Equation (4).

In Table 2, a number of examples are listed based on measured SSCCs. A correlation of the calculated Δ values given in Table 2

Table 2. Measured SSCCs $^1J(\text{CH})$ and $^1J(\text{CC})$, hybridization parameters, Fermi-contact terms $^1\text{FC}(\text{CC})$, and noncontact terms $\Delta(\text{CC})$ for some typical hydrocarbons.^[a]

Molecule	$^1J(\text{CH})$ exp	s_{CH}	sp^n_{CH}	s_{CC}	sp^n_{CC}	$s \times s \times 100$	$^1J(\text{CC})$ exp	$^1\text{FC}(\text{CC})$ calcd	Δ	$R(\text{CC})$	$\bar{p}(\text{CC})$	m
ethane	124.35	0.2487	3.021	0.2539	2.939	6.4465	34.5	34.6	−0.1	1.526	0.557	0
ethene	156.15	0.3123	2.202	0.3754	1.664	14.093	67.8	85.3	−17.5	1.339	1.390	1
acetylene	248.15	0.4963	1.015	0.5037	0.985	25.271	172.7	160.1	12.6	1.203	2.246	2
benzene	157.66	0.3153	2.171	0.3423	1.921	11.720	56.2	69.6	−13.4	1.389	0.933	0.5
allene	167.8	0.3356	1.980	0.3288	2.041	16.440	98.7	100.9	−2.2	1.306	1.451	1
propane	124.35	0.2487	3.020	0.2539	2.939	6.3297	34.6	33.9	0.7	1.523	0.557	0
cyclopropane	160.4	0.3208	2.117	0.1792	4.58	3.2113	12.4	13.2	−0.8	1.506	0.674	0
cyclobutane	133.61	0.2672	2.742	0.2328	3.296	5.4187	28.3	27.8	0.5	1.544	0.589	0
cyclopentane	128.46	0.2569	2.892	0.2431	3.114	5.9088	32.3	31.1	1.2	1.533	0.573	0
cyclohexane	124.65	0.2493	3.011	0.2507	2.983	6.2850	32.7	33.6	−0.9	1.527	0.561	0

[a] All SSCC in Hz. Experimental values are from ref. [19]. The s character s_{CH} was calculated using Equation (2b); n in sp^n_{CH} is equal to λ^2 in Equation (3); n in sp^n_{CC} was derived from the sum formula for hybrid orbitals; $^1\text{FC}(\text{CC})$ was calculated using Equation (4) ($a_{\text{CC}} = 658$; $b_{\text{CC}} = -7.9$ ^[22]) and Δ using Equation (5); the total $p(\text{CC})$ character of the C–C bond, \bar{p} , was calculated using Equation (6) where the π bond order m was derived from the number of electrons involved in π bonding. The bond lengths $R(\text{CC})$ were taken from experimental geometries where available; otherwise they were calculated at the B3LYP6–31G(d,p) level of theory.

with the C–C bond length did not lead to a significant result. A somewhat better correlation ($r^2=0.975$) was obtained when using the π -bond character as the abscissa, whereas the best result ($r^2=0.985$) was obtained when the π -bond character was replaced by the total p character, \bar{p} , of a C–C bond as given by Equation (6),

$$\bar{p} = \frac{\lambda_A^2}{\lambda_A^2 + 1} \frac{\lambda_B^2}{\lambda_B^2 + 1} + m \quad (6)$$

where m gives the π bond order. The total p character \bar{p} of Equation (6) takes into consideration that p σ orbitals also contribute to the PSO term, and therefore it should lead to a better correlation with the NC terms. Therefore, we have to distinguish in the following between the π character of a C–C bond, which matters only when a molecule contains multiple C–C bonds, and the p character of a bond, which is always larger than zero because all C–C single bonds involve p orbitals in their bond orbitals. In the following, we have to clarify whether \bar{p} is useful in connection with the interpretation of the NC terms of SSCCs $^1J(\text{CC})$. The functional dependence of the NC term Δ on \bar{p} is given by Equation (7),

$$\Delta = 33.49 \bar{p}^2 - 87.05 \bar{p} + 39.46 \quad (7)$$

(where $r^2=0.975$). Although the data of Table 2 and Figure 1 are exclusively based on measured SSCCs, in the following Sections

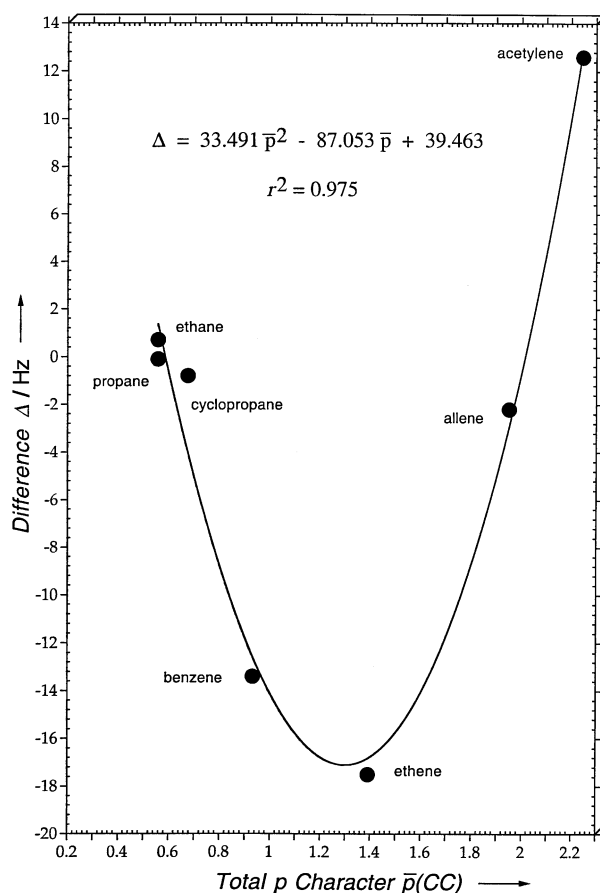
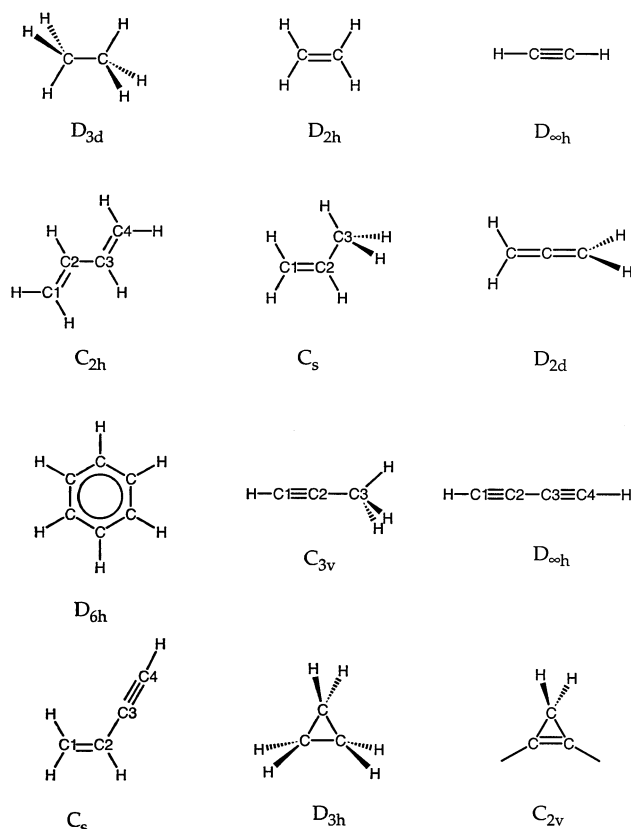


Figure 1. Functional dependence of the noncontact part Δ of $^1J(\text{CC})$ on the total p character, \bar{p} , of a C–C bond according to measured SSCCs.

we will consider the theoretical basis of correlating $^1J(\text{CC})$ with C–C bond properties in general and, in particular, test the validity of the concept derived in this Section.

3. Quantum Chemical Analysis

Coupled perturbed density functional theory (CP-DFT) was used to calculate the indirect isotropic SSCCs^[28] for a set of twelve hydrocarbons (ethane, ethene, acetylene, *trans*-1,3-butadiene, benzene, propene, allene, 1,3-butadiyne, vinylacetylene, methylacetylene, cyclopropane, and cyclopropene; see Scheme 1)



Scheme 1. Structures of the molecules investigated.

which contain typical C–C bonding situations ranging from single to triple bonds, π -conjugated and hyperconjugated bonds. For acyclic molecules, there are six different types of C–C single bond: the normal C–C bond (ethane); the two hyperconjugated C–C single bonds in propene and methylacetylene; and the three π -conjugated C–C single bonds in 1,3-butadiene, vinylacetylene, and 1,3-butadiyne. These are augmented by the two different types of C–C single bond in cyclopropane and cyclopropene (hyperconjugated C–C single bond in a strained ring). Similarly, seven different types of C–C double bond are represented by the test molecules (normal, allenic, hyperconjugated, two types of π -conjugated, aromatic, and strained). Finally, four different types of C–C triple bond were considered (normal, hyperconjugated, and two types of π -conjugated bond).

The CP-DFT calculations were carried out with the B3LYP hybrid functional^[29] and a (11s,7p,2d/6s,2p)[7s,6p,2d/4s,2p] basis set designed for the calculation of magnetic properties, especially NMR chemical shieldings.^[30] Actually, a reliable calculation of the FC term as the most important SSCC term requires the use of s-type basis functions with large exponents to describe the region close to the nucleus correctly. We have refrained from using or generating such a basis set for three reasons: 1) The basis set is chosen to be applicable to larger hydrocarbons. Because of computational limitations, this leads to some constraints concerning the size of the basis set. 2) We are interested in reproducing trends rather than accurate SSCCs. Since DFT does not account for all correlation effects, it makes no sense to use a large basis set designed for high-accuracy SSCC calculations. 3) For reasons of comparison, it is useful to employ a basis set which is also applied in the calculation of NMR chemical shifts and magnetizabilities. The SSCC calculations were carried out using, where possible, experimental geometries.^[31] A second set of calculations used B3LYP geometries obtained with the 6-31G(d,p) basis set.^[32] Differences between the SSCCs obtained with different geometries were small and will not be discussed here.

The CP-DFT/B3LYP[7s,6p,2d/4s,2p] calculations of the SSCCs led to reasonable results, which agree with the experimental $^1J(\text{CC})$ values to within 1 Hz, in the case of C–C bonds, and to within 5 Hz in the case of C=C bonds. Larger deviations were found for allene (9.3 Hz) and triple bonds (about 30 Hz). The calculated values were always larger than the measured values, which is some indirect indication of the well-known singlet–triplet instability problem, from which, in general, methods that cannot provide sufficient nondynamic electron correlation for the calculation of the SSCC, and in particular of the FC term, suffer. DFT with the approximate functionals used today has the advantage of including a large amount of unspecified nondynamic electron correlation,^[34] which helps to improve the calculation of the FC term and the total SSCC.^[28] The limitations of this description become obvious with increasing multiple bond character and reduced singlet–triplet splittings. This is reflected by the eigenvalues of the stability matrix, which are too small or even negative. Calculations can be improved by using pure exchange–correlation functionals, such as BPW91 or PW91PW91,^[33] because these functionals account in the exchange part for a larger amount of nondynamic electron correlation,^[34] which helps to describe singlet–triplet excitations more reliably.

In Figure 2, SSCCs $^1J(\text{CC})$ calculated at the CP-DFT/B3LYP[7s,6p,2d/4s,2p] level of theory are correlated with the available experimental values.^[19] The correlation coefficient r^2 is 0.999, which indicates that B3LYP provides a reliable description of the dependence of the relative magnitude of $^1J(\text{CC})$ on the nature of the C–C bond. Therefore, we refrained from additional calculations with pure DFT or the inclusion of vibrational effects, which would have led to better values for SSCCs $^1J(\text{C}\equiv\text{C})$.

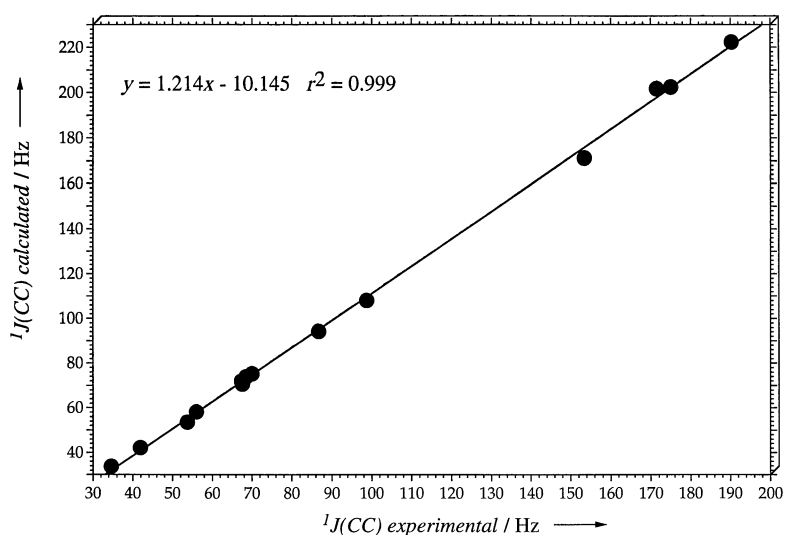


Figure 2. Correlation of calculated and experimental SSCCs $^1J(\text{CC})$. CP-DFT/B3LYP[7s,6p,2d/4s,2p] calculations.

The CP-DFT approach in the formulation of Cremer and co-workers^[28] calculates all four Ramsey terms of the SSCC, but not the individual orbital contributions leading to these terms. For this purpose, the $J\text{-OC-PSP}$ ($=J\text{-OC-OC-PSP}$: decomposition of J into orbital contributions using orbital currents and partial spin polarization) method^[25, 35, 36] was applied. The details of this method have been described elsewhere^[25, 35, 36] and therefore only some of its essentials are mentioned here.

Each SSCC can be written according to Equation (8)^[35]

$$J_{AB}^X = \sum_k^{\text{occ}} J_{A,B}^{X,k} + \sum_k^{\text{occ}} \sum_{l \neq k}^{\text{occ}} J_{A,B}^{X,k,l} \quad (8)$$

in terms of one-orbital contributions $J_{A,B}^{X,k}$ and two-orbital contributions $J_{A,B}^{X,k,l}$ defined by occupied orbitals ϕ_k and ϕ_l and the magnetic perturbation defined by operators $X = \text{FC, PSO, SD}$. Individual contributions can be determined by partial spin polarization (FC and SD) or partial induction of orbital currents (PSO and DSO) of predefined orbitals ϕ_k and ϕ_l . Of course, the individual contributions depend on the choice of the orbital, either canonical MOs, LMOs, natural LMOs (NLMOs),^[37] etc. Practice shows that LMOs lead to contributions which can be easily discussed on the basis of common chemical concepts of bonding. The localization of the orbitals was carried out with the Boys method,^[38] which localizes core and σ orbitals separately, however, in order to avoid long tails of the core orbitals and unreasonably high core contributions for the SSCCs. Also, the π orbitals were not localized, in order to distinguish between σ and π contributions. In this way, the SSCC of the CC bond can be written as in Equation (9)

$$J_{AB}^X = J_{AB}^{X,c} + J_{AB}^{X,\sigma} + J_{AB}^{X,\pi} + J_{AB}^{X,\text{ob}} + J_{AB}^{X_i(c,\sigma)} + J_{AB}^{X_i(c,\pi)} + J_{AB}^{X_i(c,\text{ob})} + J_{AB}^{X_i(\sigma,\pi)} + J_{AB}^{X_i(\sigma,\text{ob})} + J_{AB}^{X_i(\pi,\text{ob})} \quad (9)$$

where σ , π , and c denote $C_A C_B$ σ -bond and π -bond LMOs as well as C_A or C_B core (c) LMOs directly associated with the coupling

nuclei. The coupling mechanism can also involve other bonds (ob) attached to the two carbon nuclei in question, which have also to be included in Equation (9), thus yielding four different types of one-orbital contributions for each Ramsey term, in the case of a general C–C bond with multiple-bond character. For the FC, PSO, and SD terms, there are also six different types of two-orbital contributions, see Equation (9). A two-orbital contribution itself is the sum of two different terms: $(k,l) = (k \leftarrow l) + (l \leftarrow k)$, which indicates that the perturbation can be on orbital l —leading to first-order orbital k —or, alternatively, it can be on orbital k —leading to first-order orbital l . The ten different types of orbital contributions in Equation (9) were determined from a contraction of maximally 81 individual orbital contributions in the case of a general C–C single bond with six different substituents, 64 in the case of a general C=C double bond, and 36 in the case of a general C≡C triple bond. These terms were calculated at the same time and contracted by the *J*-OC-PSP method.

One can directly predict the sign and magnitude of $J_{AB}^{FC,k} = FC(k)$ or $J_{AB}^{FC,(k,l)} = FC(k,l)$ when considering graphical representations of the appropriate zeroth- and first-order orbitals.^[25, 35] The sign of these orbitals at the positions of the coupling nuclei determines the sign of the FC spin density distribution at these locations and by this the sign of the FC orbital contribution. The FC term can be expressed as a function of the spin density at the responding nucleus A, as shown in Equation (10)

$$FC(AB) = \frac{4}{3} \gamma_A \gamma_B \alpha^2 \rho^{(B),FC}(\mathbf{R}_A) \quad (10)$$

where γ_A is the gyromagnetic ratio of nucleus A; α is Sommerfeld's fine-structure constant; and \mathbf{R}_A is the position vector for nucleus A. The first-order density $\rho^{(B),FC}$ (also called the Fermi-contact spin-density distribution^[25]), is given by Equation (11)

$$\rho^{(B),FC}(\mathbf{r}) = 2 \sum_k^{\text{occ}} \sum_{\sigma} \psi_{k\sigma}^{(0)}(\mathbf{r}) \psi_{k\sigma}^{(B),FC}(\mathbf{r}) \quad (11)$$

where σ denotes the spin variable, $\psi_{k\sigma}^{(0)}$ the zeroth-order orbital, and $\psi_{k\sigma}^{(B),FC}$ the first-order spin orbital; the orbital index k runs over all occupied (occ) orbitals. The Fermi-contact spin density can be split into one- and two-orbital contributions in the same way as the total SSCC—see Equations (8) and (9)—which is utilized in the *J*-OC-PSP approach.^[35] One can plot the Fermi-contact spin density for each orbital term and determine the sign of the FC term by inspection of the spin density at the coupling nuclei: a dominance of β -spin density ($\rho^{(B),FC}(\mathbf{R}_B) < 0$) at the perturbed nucleus and α -spin density ($\rho^{(B),FC}(\mathbf{R}_A) > 0$) at the responding nucleus leads to a positive FC term; a dominance of β -spin density (or α -spin density) at both nuclei leads to a negative FC term. Similar relationships can be derived for the PSO, SD, and DSO contributions, and has been discussed elsewhere.^[25, 35, 36, 39]

The sign of the Fermi-contact spin density can be anticipated by inspecting the zeroth-order LMO l and the first-order LMO k . It has been shown that their nodal behavior, and by this the sign of their amplitudes at the nuclei, can be predicted once these orbitals have been plotted for a representative case.^[25] Hence,

we will use graphical representations of zeroth-order orbitals, first-order orbitals, and the Fermi-contact spin density distribution to rationalize calculated orbital contributions. All SSCC calculations and graphical representations have been carried out with the quantum chemical program package COLOGNE 2003.^[40]

4. Results and Discussion

In Table 3, the SSCCs $^1J(\text{CC})$ of the hydrocarbons shown in Scheme 1 (except cyclopropane and cyclopropene) are decomposed into their Ramsey terms, and each Ramsey term is decomposed into one-orbital and two-orbital terms according to *J*-OC-PSP calculations.^[25, 35] Since the DSO contributions to the total SSCC are small, we refrained from documenting and analyzing these terms. The orbital contributions determined by *J*-OC-PSP reproduce exactly the total SSCC, and therefore the DSO contributions can be obtained by subtracting the three Ramsey terms documented from the total SSCC. To simplify the notation of orbital terms, we used the following symbols: The orbital contribution $FC[\sigma(\text{CC})]$ has to be distinguished from the total term $FC(\text{CC})$; also the two-orbital term $FC[c, \sigma(\text{CC})]$ from the individual two-orbital contributions $FC[c \leftarrow \sigma(\text{CC})]$ and $FC[\sigma(\text{CC}) \leftarrow c]$. If we want to distinguish, in the set of all calculated $FC(\text{CC})$ terms, those associated with C–C single bonds from those associated with C–C double bonds, we will use the notation $FC(\text{C–C})$ and $FC(\text{C=C})$ (similarly $FC[\sigma(\text{C–C})]$ and $FC[\sigma(\text{C=C})]$).

As shown in Figure 2, calculated and experimental SSCC values^[19] are in reasonable agreement, reproducing all trends in total and partial SSCCs correctly. Differences between calculated and measured SSCCs result from four different reasons: 1) correlation effects are not accounted for by DFT; 2) the use of too small a basis set; 3) rovibrational effects are contained in measured SSCCs $^1J(\text{CC})$ —these are particularly large for C–C triple bonds;^[41] and 4) experimental SSCCs also cover environmental effects because they have been measured mostly in solution.

In the following, we will discuss the FC and NC terms, their orbital contributions, and their relationship to other C–C bonding properties. For this purpose, besides the C–C bond length we have also determined C–C bond orders, in three different ways. First, we used Weinhold's approach to calculate the C–C bond order as a *natural bond order* based on his natural resonance theory (NRT).^[42] These bond orders are called NRT bond orders. We also employed the AOM (atomic overlap matrix) bond orders of Cioslowski and Mixon,^[43] which are based on the virial partitioning method of Bader.^[44] Finally, we used the definition for the p character, \bar{p} , of a C–C bond given in Equation (6) to analyze the NC terms. For this purpose, we determine λ_A^2 and λ_B^2 using natural bond orbitals (NBOs).^[37] The π bond order of a multiple C–C bond was calculated using both Hückel, NRT, and AOM bond orders. The latter provided a consistent description (see below) and will be exclusively used in this work. Bond orders and adiabatic frequencies were calculated at the B3LYP6–31G(d,p) level of theory.^[29, 32] They are listed in Table 4.

Table 3. Decomposition of calculated $^1J(\text{CC})$ constants for some typical hydrocarbons.^[a]

Type	C_2H_6 , C1-C2				C_2H_4 , C1=C2				C_2H_2 , $\text{C1}\equiv\text{C2}$				Benzene			
	PSO	FC	SD	$^1J(\text{CC})$	PSO	FC	SD	$^1J(\text{CC})$	PSO	FC	SD	$^1J(\text{CC})$	PSO	FC	SD	$^1J(\text{CC})$
c		0.13		0.13		3.20		3.19	−0.01	4.53		4.54		1.17		1.17
$\sigma(\text{ob})$	0.65	−25.90	0.26	−24.71	−1.30	−35.21	−0.22	−36.51	−1.37	−70.15	−0.51	−71.95	−0.77	−34.40	−0.07	−34.90
$\sigma(\text{CC})$	−0.66	105.44	0.75	105.39	−5.03	170.81	−0.38	165.21	−6.53	313.05	−0.94	305.44	−3.45	152.03	0.02	148.43
$\pi(\text{CC})$				−2.04			5.31	3.31	18.31		13.40	31.84	−1.73		1.80	0.14
$[\text{c},\sigma(\text{ob})]$		0.51		0.52	0.01	−11.50	−0.01	−11.50	0.01	−19.15	−0.01	−19.15	0.01	−5.44		−5.44
$[\text{c},\sigma(\text{CC})]$		−12.67	0.01	−12.67	−0.01	−11.34	−0.01	−11.36	−0.01	−0.69	−0.01	−0.71	−0.01	−9.47		−9.47
$[\text{c},\pi(\text{CC})]$							0.07	0.07			0.17	0.17		0.01	0.02	0.03
$[\sigma(\text{ob}),\sigma(\text{CC})]$	0.02	−35.00	0.06	−34.92	−1.62	−39.07	−0.32	−41.01	−1.80	−45.93	−0.36	−48.08	−0.99	−40.04	−0.13	−41.15
$[\sigma(\text{ob}),\pi(\text{CC})]$				−0.03			−0.11	−0.14	−0.06	0.01	0.07	0.02	−0.05		−0.06	−0.11
$[\sigma(\text{CC}),\pi(\text{CC})]$				−0.26			−0.38	−0.63	−0.16		−0.22	−0.38	−0.20		−0.29	−0.49
$^1J(\text{CC})$	0.02	32.50	1.08	33.74	−10.28	76.88	3.94	70.62	8.38	181.67	11.60	201.73	−7.19	63.87	1.29	58.21
Exp.				34.6				67.6				171.5				56.0
Type	Propene, $\text{C}_1=\text{C}_2$				Propene, C_2-C_3				Methylacetylene, $\text{C}_1\equiv\text{C}_2$				Methylacetylene, C_2-C_3			
	PSO	FC	SD	$^1J(\text{CC})$	PSO	FC	SD	$^1J(\text{CC})$	PSO	FC	SD	$^1J(\text{CC})$	PSO	FC	SD	$^1J(\text{CC})$
c		3.00		3.00		0.13		0.13	−0.03	4.37		4.38	−0.02	−0.04		−0.04
$\sigma(\text{ob})$	−1.29	−36.30	−0.10	−37.42	−1.15	−29.73	0.01	−30.59	−1.21	−71.00	−0.38	−72.46	−0.92	−37.00	−0.01	−37.73
$\sigma(\text{CC})$	−4.97	174.94	−0.37	169.42	−1.12	125.32	0.63	124.66	−6.35	312.10	−0.92	304.70	−1.27	172.31	0.40	171.34
$\pi(\text{CC})$	−1.83		4.62	2.93	1.14		0.07	1.25	17.53		12.52	30.18	0.52		0.11	0.73
$[\text{c},\sigma(\text{ob})]$	0.01	−11.31		−11.31		−0.60		−0.60	0.01	−18.86		−18.86		−2.97		−2.97
$[\text{c},\sigma(\text{CC})]$	−0.01	−10.41	−0.01	−10.42		−11.96	0.01	−11.95	−0.01	−0.10	−0.02	−0.13		−9.27		−9.27
$[\text{c},\pi(\text{CC})]$			0.06	0.06							0.16	0.16				
$[\sigma(\text{ob}),\sigma(\text{CC})]$	−1.58	−38.76	−0.33	−40.67	−0.20	−40.60		−40.81	−1.73	−43.65	−0.34	−45.7	−0.23	−50.01	−0.02	−50.25
$[\sigma(\text{ob}),\pi(\text{CC})]$	−0.04		0.25	0.22	−0.02		0.09	0.07	0.15		0.40	0.55	0.20		0.13	0.33
$[\sigma(\text{CC}),\pi(\text{CC})]$	−0.23		−0.34	−0.57	0.02		−0.06	−0.04	−0.16		−0.20	−0.36	0.01		−0.16	−0.15
$^1J(\text{CC})$	−9.94	81.17	3.78	75.15	−1.34	42.55	0.75	42.12	8.21	182.86	11.22	202.41	−1.70	73.02	0.42	71.89
Exp.				70.0				41.9				175.0				67.4
Type	<i>trans</i> -1,3-Butadiene, C2-C3				<i>trans</i> -1,3-Butadiene, C1=C2				1,3-Butadiyne, $\text{C1}\equiv\text{C2}$				1,3-Butadiyne, C2-C3			
	PSO	FC	SD	$^1J(\text{CC})$	PSO	FC	SD	$^1J(\text{CC})$	PSO	FC	SD	$^1J(\text{CC})$	PSO	FC	SD	$^1J(\text{CC})$
c		0.62		0.62		3.05		3.05	−0.01	4.87		4.87	0.01	0.73		0.74
$\sigma(\text{ob})$	−0.20	−36.00	0.08	−35.82	−1.13	−34.53	−0.17	−35.55	−1.13	−63.47	−0.42	−64.90	0.12	−51.61	−0.06	−51.37
$\sigma(\text{CC})$	−1.65	149.79	0.46	148.44	−4.81	170.77	−0.32	165.46	−6.22	319.80	−0.88	312.53	−1.95	271.94	0.09	269.92
$\pi(\text{CC})$	−0.73		0.97	0.31	−2.02		5.04	3.07	17.22		13.39		30.76	−0.44		1.94
$[\text{c},\sigma(\text{ob})]$		−3.38		−3.37	0.01	−11.24	−0.01	−11.24	0.01	−18.95	−0.01	−18.95	0.01	−8.53		−8.52
$[\text{c},\sigma(\text{CC})]$		−11.04	0.01	−11.04	−0.01	−10.81	−0.01	−10.83	−0.01	−1.33	−0.01	−1.36	−0.01	−0.88		−0.88
$[\text{c},\pi(\text{CC})]$		0.05	0.01	0.06			0.06	0.06		−0.01	0.17	0.16			0.02	0.02
$[\sigma(\text{ob}),\sigma(\text{CC})]$	−0.27	−44.88	0.07	−45.08	−1.51	−37.56	−0.29	−39.36	−1.56	−38.58	−0.29	−40.44	−0.25	−39.59	0.04	−39.80
$[\sigma(\text{ob}),\pi(\text{CC})]$	−0.03		−0.06	−0.09	−0.03		−0.12	−0.14	−0.07		0.03	−0.04	−0.05		−0.07	−0.12
$[\sigma(\text{CC}),\pi(\text{CC})]$	−0.09		−0.24	−0.33	−0.25		−0.37	−0.62	−0.17		−0.24	−0.41	−0.08		−0.35	−0.43
$^1J(\text{CC})$	−2.96	55.06	1.29	53.60	−9.75	79.68	3.82	73.91	8.06	202.35	11.73	222.26	−2.66	172.04	1.62	171.22
Exp.				53.7				68.6				190.3				153.4
Type	$\text{H}_2\text{C}=\text{CH}-\text{C}\equiv\text{CH}$, C1=C2				$\text{H}_2\text{C}=\text{CH}-\text{C}\equiv\text{CH}$, C2-C3				$\text{H}_2\text{C}=\text{CH}-\text{C}\equiv\text{CH}$, $\text{C3}\equiv\text{C4}$				Allene, C1=C2			
	PSO	FC	SD	$^1J(\text{CC})$	PSO	FC	SD	$^1J(\text{CC})$	PSO	FC	SD	$^1J(\text{CC})$	PSO	FC	SD	$^1J(\text{CC})$
c	−0.03	3.29		3.29	−0.04	0.43		0.43	−0.03	4.55		4.56		2.86		2.86
$\sigma(\text{ob})$	−1.01	−30.07	−0.17	−31.01	−0.43	−39.26	0.01	−39.49	−1.16	−68.61	−0.38	−70.04	1.35	−38.46	0.52	−36.37
$\sigma(\text{CC})$	−4.60	164.51	−0.32	159.42	−1.69	195.62	0.27	194.03	−6.28	309.77	−0.89	302.46	−4.70	208.73	−0.41	203.43
$\pi(\text{CC})$	−2.46	−0.04	5.38	2.93	−0.27		0.86	0.73	16.91		12.66	29.70	−3.16		3.74	0.68
$[\text{c},\sigma(\text{ob})]$	0.01	−11.57	−0.01	−11.57	0.01	−5.19		−5.19	0.01	−19.11		−19.10	0.01	−11.64	0.01	−11.63
$[\text{c},\sigma(\text{CC})]$	−0.01	−10.84	−0.01	−10.85	−0.01	−8.15		−8.15	−0.01	−1.04	−0.01	−1.06	−0.01	−8.12	−0.01	−8.13
$[\text{c},\pi(\text{CC})]$		−0.64	0.07	−0.57			0.01	0.01			0.16	0.16		0.03	0.05	0.08
$[\sigma(\text{ob}),\sigma(\text{CC})]$	−1.33	−34.45	−0.26	−36.04	−0.27	−47.67	0.01	−47.92	−1.69	−41.59	0.33	−43.61	−1.30	−41.42	−0.28	−42.99
$[\sigma(\text{ob}),\pi(\text{CC})]$	−0.06	0.64	−0.13	0.46	0.02		0.06	0.08	0.09		0.30	0.39	0.08		0.57	0.65
$[\sigma(\text{CC}),\pi(\text{CC})]$	−0.32	1.87	−0.38	1.17	−0.05		−0.28	−0.33	−0.16		−0.23	−0.39	−0.18		−0.35	−0.53
$^1J(\text{CC})$	−9.80	82.71	5.51	77.23	−2.74	95.78	0.94	94.19	7.67	183.98	11.28	203.06	−7.90	111.94	3.84	108.00
Exp.								86.7								98.7

[a] All SSCC and SSCC contributions in Hz. Experimental values from ref. [19] CP-DFT/B3LYP[7s,6p,2d/4s,2p] calculations. For atom numbering, compare with Scheme 1. Values smaller than $|0.01|$ are not shown. For an explanation of orbital contributions, see text.

Table 4. Comparison of different calculated C–C bond properties for some typical hydrocarbons.^[a]

Molecule	Bond	$R(\text{CC})$ [Å]	\bar{p} Character	NRT Bond order	AOM Bond order	ω_a [cm ⁻¹]	$s_A \times s_B$ Character	Δ [Hz]
ethane	C–C	1.530	0.552	1.024	1.035	1083	0.079	1.24
ethene	C=C	1.330	1.316	2.023	1.947	1674	0.153	– 6.26
acetylene	C≡C	1.206	2.134	2.994	2.902	2234	0.268	20.06
benzene	C…C	1.396	0.847	1.493	1.427	1366	0.124	– 5.66
propene	C1=C2	1.333	1.286	1.986	1.919	1658	0.155	– 6.02
propene	C2=C3	1.502	0.541	1.024	1.061	1130	0.094	– 0.43
allene	C1=C2	1.306	1.273	1.991	1.962	1729	0.185	– 3.94
1,3-butadiene	C2=C3	1.457	0.563	1.061	1.114	1207	0.1085	– 1.46
1,3-butadiene	C1=C2	1.340	1.243	1.939	1.869	1622	0.151	– 5.77
1,3-butadiyne	C1≡C2	1.212	1.978	2.859	2.749	2172	0.272	19.91
1,3-butadiyne	C2=C3	1.369	0.427	1.115	1.237	1474	0.219	– 0.82
vinylacetylene	C1=C2	1.341	1.232	1.942	1.859	1619	0.151	– 5.48
vinylacetylene	C2=C3	1.424	0.500	1.066	1.145	1289	0.153	– 1.59
vinylacetylene	C3≡C4	1.211	2.013	2.903	2.782	2190	0.269	19.08
methylacetylene	C1≡C2	1.207	2.071	2.943	2.802	2216	0.271	19.55
methylacetylene	C2=C3	1.460	0.225	1.039	1.095	1219	0.13	– 1.13
cyclopropane	C1–C2	1.508	0.640	0.997	1.028	1082	0.047	– 0.93
cyclopropene	C1–C2	1.509	0.650	1.002	1.050	1065	0.050	– 1.08
cyclopropene	C1=C3	1.295	1.360	1.964	1.950	1786	0.129	– 1.39

[a] Bond lengths $R(\text{CC})$, p character \bar{p} , bond orders NRT and AOM, and adiabatic C–C stretching frequencies were calculated at the B3LYP/6-31G(d,p) level of theory, noncontact terms Δ at CP-DFT/B3LYP/[7s,6p,2d/4s,2p]. 1,3-Butadiene was calculated in the *trans* conformation.

A bond property such as the bond length or the dissociation energy reflects to a different degree the influence of the substituents on a bond, which, via nonbonded interactions, can stabilize or destabilize a bond. The SSCC is very sensitive to substituent effects, as we will see in the following discussion. Therefore, it was appropriate to have, in addition to the bond length R , another bond property whose sensitivity to substituent effects equals that of the SSCC. For this purpose, we chose the adiabatic stretching frequency ω_a of the C–C bond invented by Konkoli and Cremer.^[45] The adiabatic vibrational modes are localized modes, the properties of which (force constant and frequency) can be used to describe a chemical bond.^[46]

4.1. Total $^1J(\text{CC})$ Coupling Constants

It has been speculated that $^1J(\text{CC})$ is a reasonable descriptor of the C–C bond and correlates with C–C bond lengths and C–C stretching force constants.^[21] Indeed, by considering just the typical C–C single (ethane), double (ethene), and triple bond (acetylene), this relationship seems to be fulfilled. However, as soon as a larger set of C–C bonds is considered, neither bond length R , adiabatic stretching frequencies, nor bond orders VRT and AOM correlate with $^1J(\text{CC})$ (either calculated or measured). In particular, for the conjugated or hyperconjugated CC single bonds in 1,3-butadiyne, 1,3-butadiene, vinylacetylene, and methylacetylene, the SSCC $^1J(\text{CC})$ is much larger than expected. This is also true for the C–C double bond in allene, which, by hyperconjugation, gets some triple bond character. It seems that $^1J(\text{CC})$ is sensitive to electronic effects, which are not reflected by other bond properties, such as bond length, adiabatic stretching frequency, or bond order. In the following, we will analyze the difference between SSCCs $^1J(\text{CC})$ and other properties when describing CC bonds.

4.2. Fermi-Contact Contributions

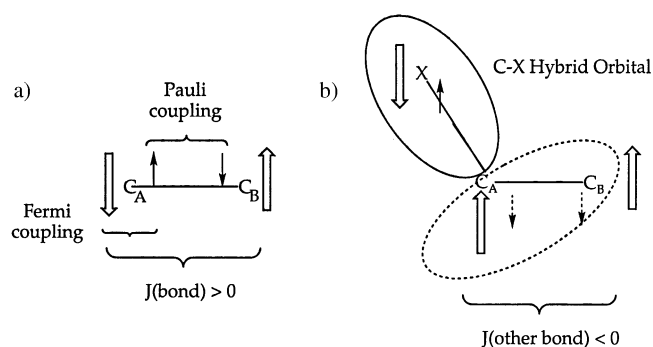
The failure to describe the character of a C–C bond with $^1J(\text{CC})$ becomes immediately clear upon recognizing that all $^1J(\text{CC})$ values are largely dominated by the FC term. The FC term probes the spin density at the contact surface of the coupling nuclei and in this way it is a local property, which can hardly describe the bond density and by this the character of the chemical bond. It has been argued that the FC term reflects the s density at the nucleus, which in turn depends on the nature of the hybrid orbitals forming the C–C bond. Therefore, the FC term should reflect the nature of the C–C bond. These arguments have to be corrected in several ways. First, the FC term depends on the spin density rather than the density itself. Hence, a correlation of the FC term with the s character will only be successful if the (zeroth-order) s density and (first-order) s spin density at the nucleus correlate with each other, which is by no means guaranteed because the former depends on the electronegativity of the atom and its valence state in question, whereas the latter depends on the polarizability of the density. Second, the FC term is dominated by the $\text{FC}[\sigma(\text{CC})]$ contribution (Table 3), however relatively large negative contributions of all substituent bond orbitals (one- and two-orbital terms involving $\sigma(\text{ob})$ in Table 3) add to the value of the FC term. These orbital contributions do not correlate with either the term $\text{FC}[\sigma(\text{CC})]$ or the product of the s-characters $s_A \times s_B$ of the C–C bond (see Table 4). Therefore, one cannot expect a satisfactory correlation between $^1J(\text{CC})$ or $^1\text{FC}(\text{CC})$ and the s character of the C–C bond, contrary to what is often claimed in the literature. To clarify this point in more detail, we will investigate trends in the calculated FC terms further.

The largest FC contribution is that of the $\sigma(\text{CC})$ orbital. It increases from 105 Hz for ethane to 171 Hz for ethene and 313 Hz for acetylene (Table 3). Hyperconjugation, as it occurs in

propene, leads to 125 Hz for the C–C single bond and 175 Hz for the C–C double bond. In the case of conjugated π bonds, intermediate values of 150 (C2–C3 bond in butadiene) and 152 Hz (CC bond in benzene) were calculated (Table 3). However, for the formal single bond C2C3 in 1,3-butadiyne, a value of 272 Hz was obtained, which, even if it were too large by 30 Hz, is still unusual in view of the other values. The sensitivity of $FC[\sigma(CC)]$ is low in the case of the different double bonds (170.8 versus 170.8 in the case of ethene and the C1C2 bond of *trans*-1,3-butadiene) or different formal single bonds (150 and 152 Hz respectively for C2C3 in butadiene and the benzene C–C bond); They hardly vary, although other bond properties, such as bond length and bond stretching frequency (Table 4) clearly show the difference of these bonds.

The total FC terms are much smaller (30 to 60%) than the $\sigma(CC)$ LMO contributions. As in the case of the correlation between calculated and measured $^1J(CC)$ values ($r^2 = 0.999$, Figure 2), the FC term and $FC[\sigma(CC)]$ correlate with each other in a linear fashion, however, the correlation coefficient ($r^2 = 0.988$) is smaller. This is a consequence of the fact that σ_{CH} , or in general other bond contributions, are negative (Table 3). In Figure 3, zeroth-order LMO(CC), first-order LMO(CC), and the Fermi-contact spin density of the CC coupling constant in ethane are shown for the contributions $\sigma(CC)$ and $\sigma(CH)$. The zeroth-order LMO $\sigma(CC)$ is formed by two sp^3 -type hybrid orbitals in a bonding overlap, so that the LMO $\sigma(CC)$ gets two nodal surfaces. The carbon nuclei are both positioned in the back lobes of the corresponding hybrid orbitals. Since the perturbation is at C_B , the first-order orbital possesses a strong admixture of the $\sigma(CC)$ -orbital, and an additional nodal surface between the coupling carbon nuclei (surrounding nucleus C_B ; Figure 3b). In this way, the Fermi-contact spin density distribution (Figure 3c) obtains different signs at the nuclei, thus leading to a positive $FC[\sigma(CC)]$ orbital contribution.

The results of an analysis of zeroth- and first-order orbital and the corresponding FC spin density distribution can be summarized in a Dirac vector model (see Scheme 2a). Assuming that



Scheme 2. Dirac vector model (a) and extended Dirac vector model (b) for two-orbital contributions to the FC term of $^1J(C_A-C_B)$. a) Sign of the bond orbital contribution. b) Sign of a bond orbital contribution leading to a substituent X (other bond). The C–X hybrid orbital is schematically given where the tail is enlarged to indicate that it encompasses the C_A-C_B bond. The nuclear spin is given by large arrows, the electron spin by small arrows.

nucleus C_B has α -spin, Fermi coupling will lead to a dominance of β -spin density at C_B , that is, the bond electron next to nucleus C_B possesses preferably β -spin and the FC spin density is negative. Pauli coupling (electron-pair coupling) will imply that the bonding electron close to nucleus C_A will preferably adopt α spin, which in turn will lead to β -spin for the spin moment of nucleus C_A via Fermi coupling. In this way, the two carbon nuclei possess the right spin momenta for a positive NMR SSCC. The contribution $\sigma(CC)$ becomes positive, as indicated by the Dirac vector model of Scheme 2a.

In the case of the LMOs describing bonding to substituents X (H or C), nucleus C_B is located in the positive back lobe of LMO(C–X), whereas C_A is positioned in a negative orthogonalization tail (Figure 3d). The first-order LMO(C–X) has a similar form to the first-order LMO(C–C), that is, there is an additional nodal surface at the center of the C–C bond, which leads to a positive amplitude on nucleus C_A and a negative amplitude at C_B (Figure 3e). The combination of the amplitudes gives a negative FC spin density (dominance of β -spin) at the coupling nuclei, both nuclei adopt α -spin by Fermi coupling, thus leading to a negative C–X bond LMO contribution to the FC term (Figure 3f). The magnitude of the ob orbital contributions increases with the s spin density at the nuclei. This increases from a single to a double and to a triple C–C bond because both the electronegativity and polarizability increase from an sp^3 to an sp^2 and to an sp hybrid orbital. For the six C–H bonds of ethane, we obtain -25.9 , for the four C–H bonds of ethene -35.2 , and for the two CH bonds of acetylene a -70 Hz contribution to $^1FC(CC)$, corresponding to -4.3 , -8.8 , and -35.1 Hz per C–H bond in the three molecules. These values change, however, when the C–H bond is replaced by a second C–C bond, or the ethene C–C bond is replaced by the C–C bond in benzene.

There are two-orbital contributions to the FC term, which involve either the $\sigma(CC)$, $\sigma(ob)$, or both LMOs. The two-orbital contributions correspond to steric exchange interactions leading to relatively strong spin polarization at the coupling nuclei. All these contributions are negative, which can easily be explained with the help of zeroth-order and first-order orbitals, or the FC spin density distribution resulting from them.^[25] Some of these contributions, such as $[\sigma(CC), \sigma(ob)]$ do not change much, others do (Table 3). There are negative two-orbital contributions involving the core (c) orbitals. One-orbital c-contributions are negligible because a c-orbital located at C_B (C_A) has a vanishingly small amplitude at C_A (C_B) and therefore cannot support any significant spin polarization at the two nuclei. This holds also for the $(\sigma(CC), c)$ contributions, however, not for the $[c, \sigma(CC)]$ contributions, since a first-order c-orbital gets an admixture from the $\sigma^*(CC)$ orbital and therefore possesses finite amplitudes at the coupling nuclei.

The one- and two-orbital ob contributions reduce the bond-contribution substantially, so that the trend in the total FC term is no longer determined solely by the $\sigma(CC)$ part, although this is still the most important term. Clearly, the FC coupling mechanism depends on both the nature of the CC bond and the nature of the substituent bonds. This will become understandable if one considers that it is not only the bonding LMO that determines the density in the bond region and the bond strength, but it is

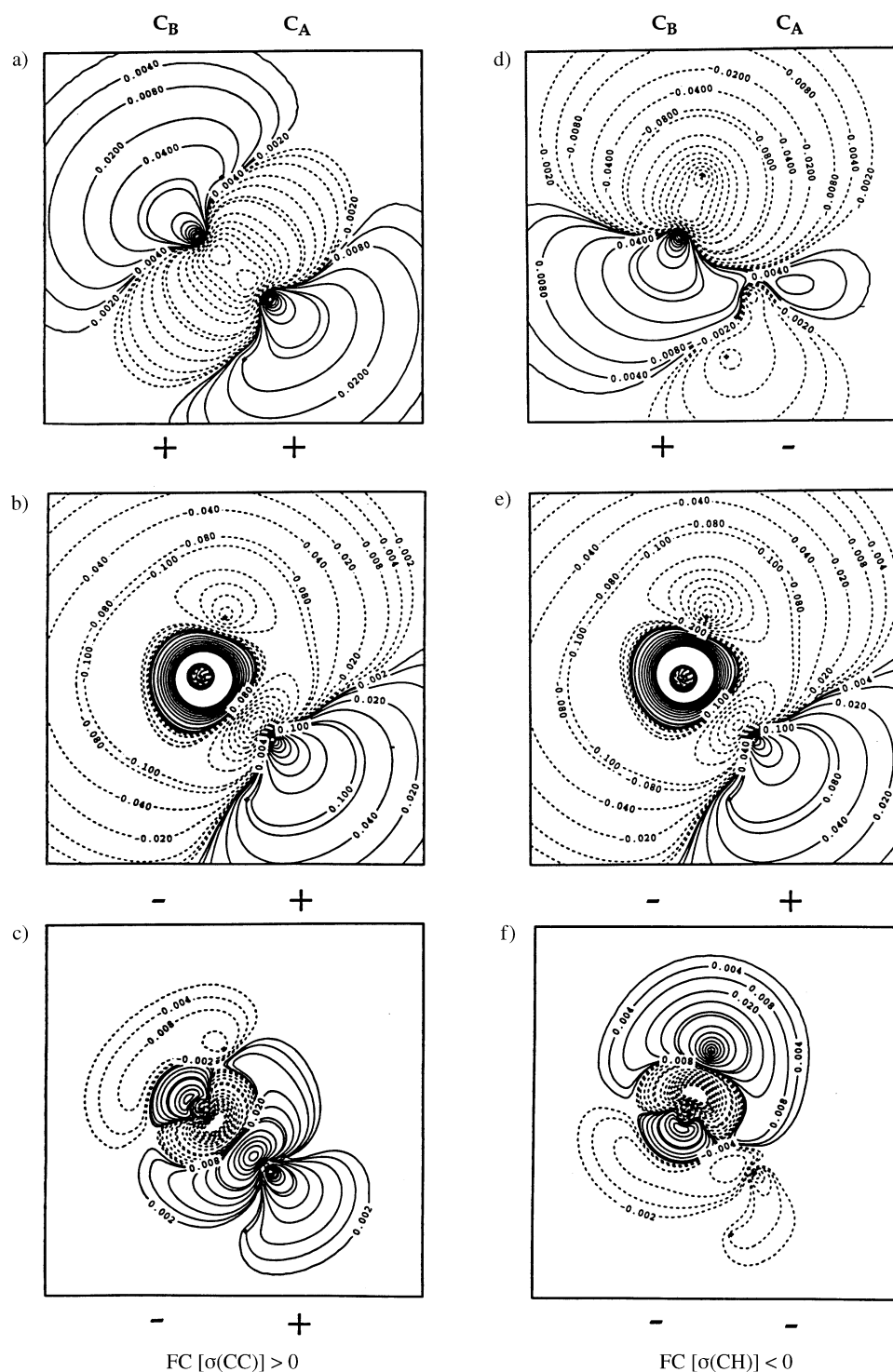


Figure 3. Explanation of the sign of the orbital terms contributing to the SSCC ${}^1J(CC)$ in staggered ethane. Contour line diagrams of a) the zeroth-order C–C bonding LMO of staggered ethane, b) the first-order C–C bonding LMO (perturbation at C_B), c) the FC spin density distribution of the bonding C–C orbital, d) the zeroth-order C–H bonding LMO of staggered ethane, e) the first-order C–H bonding LMO (perturbation at C_B), and f) the FC spin density distribution of the bonding C–H orbital. Nucleus C_A is at the lower right part, nucleus C_B at the upper left part of the drawing. The C–H bond considered is C_B –H and extends to the upper middle of the drawing. Solid contour lines indicate a positive orbital amplitude (positive spin density distribution, that is, more α density), dashed contour lines a negative orbital amplitude (negative spin density distribution, that is, more β density). The sign of the LMO amplitude or the value of the FC spin density distribution at the coupling nuclei is given as well as the sign of the corresponding orbital contribution to ${}^1J(CC)$. CP-DFT/B3LYP[7s,6p,2d/4s,2p] calculations.

also the ob-LMOs via their tails, which envelop the two carbon atoms and add to the bond density via their tail-densities (Figure 3d). For the two-orbital contributions that represent

steric repulsion, the same is true. As far as there is a mutual penetration of densities (equivalent to a repulsion of substituent bonds), this leads to a weakening of the C–C bond.

In previous work, the magnitude of the FC term was estimated from the s densities at the coupling nuclei by utilizing the product $\rho_s^{(I,J)}(A,B) = \rho_s^I(A)\rho_s^J(B)$ where the s density is evaluated for the LMO ϕ_i at the coupling nucleus N , as shown in Equation (12),

$$\rho_s^I(N) = \langle \phi_i | \delta(\mathbf{r}_N) | \phi_i \rangle \quad (12)$$

where $\delta(\mathbf{r}_N)$ is the Dirac delta function. In view of the present discussion, this is a simplification originally often based on semiempirical FPT-INDO theory,^[47, 48] which did not provide accurate FC(CC) values. However, early experimental investigations on the dependence of the SSCC $^1J(\text{CC})$ on the s character of the C–C bond showed that relationships such as Equation (4) hold only for a limited set of well-defined C–C bonds. For example, we find that the calculated $^1\text{FC}(\text{CC})$ values correlate poorly with the calculated s character ($r^2 = 0.971$; Figure 4a) whereas the linear correlation can be considerably improved if just the $\sigma(\text{CC})$ orbital contribution is considered for the six different types of C–C single bonds ($r^2 = 0.996$; Figure 4a). In this way, the “noise” generated by the negative orbital contributions is suppressed. A similar linear correlation for the formal C–C double bonds leads, however, to a less useful result ($r^2 = 0.979$; Figure 4a). The actual double bond values calculated for ethene, propene, *trans*-1,3-butadiene, and vinylacetylene cluster in a narrow range (see also Tables 3 and 4) and the correlation obtained does not provide a useful differentiation of these bonds. The triple bond values are positioned neither on the correlation line for C–C single bonds nor on that for C–C double bonds. The observations made for the $\sigma(\text{CC})$ orbital contribution applies also to the total FC values. For a s -character typical of C–C triple bonds, the FC terms predicted by the linear correlation found for C–C single bonds differ by 60 Hz from those predicted by the linear correlation for double bonds. In general, relationships such as Equation (4) are not valid for C–C bonds.

The conclusion drawn on the basis of Figure 4a can be verified by correlating FC contributions with typical bond properties such as the C–C bond length or adiabatic stretching frequency. In Figure 4b, the total FC terms and the $\text{FC}[\sigma(\text{CC})]$ orbital contributions are described as an exponential fit of the bond length $R(\text{CC})$. Poor correlations were obtained ($r^2 = 0.787$ and 0.776 ; solid lines in Figure 4b), which were again substantially improved if just C–C single or double bonds are considered (dashed lines in Figure 4b). These correlations magnify those trends already found in connection

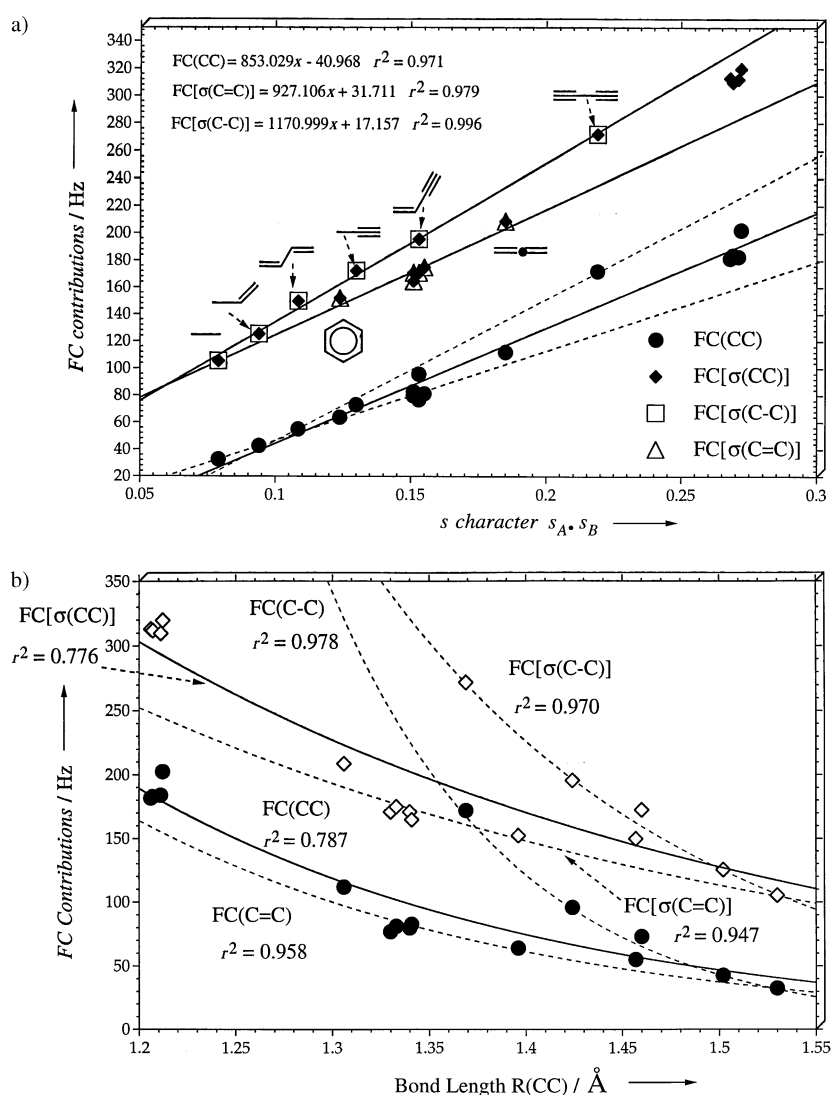


Figure 4. Use of the FC term for describing properties of the C–C bond. a) Dependence of calculated total $^1\text{FC}(\text{CC})$ values and $\text{FC}[\sigma(\text{CC})]$ orbital contributions on the s character $s_A \times s_B$ of the C–C bond. Different linear correlations are tried: 1) Correlation of all $^1\text{FC}(\text{CC})$ terms (—; ●; $r^2 = 0.971$). 2) Correlation of the $\text{FC}(\text{CC})$ terms calculated for formal C–C single bonds ($\text{FC}(\text{C}-\text{C})$; upper ---; ●; $r^2 = 0.978$). 3) Correlation of the $\text{FC}(\text{CC})$ terms calculated for formal C–C double bonds ($\text{FC}(\text{C}=\text{C})$; lower ---; ●; $r^2 = 0.958$). 4) Correlation of the $\text{FC}[\sigma(\text{CC})]$ terms calculated for formal C–C single bonds ($\text{FC}[\sigma(\text{C}-\text{C})]$; upper ---; □; $r^2 = 0.996$). 5) Correlation of the $\text{FC}[\sigma(\text{CC})]$ terms calculated for formal C–C double bonds ($\text{FC}[\sigma(\text{C}=\text{C})]$; middle ---; △; $r^2 = 0.979$). For values see Tables 3 and 4. b) Dependence of the calculated total $^1\text{FC}(\text{CC})$ values (●) and $\text{FC}[\sigma(\text{CC})]$ orbital contributions (◇) on the C–C bond length R . Six different exponential correlations are considered: 1) all $^1\text{FC}(\text{CC})$ values (lower —; ●; $r^2 = 0.787$); 2) $^1\text{FC}(\text{CC})$ values for formal C–C single bonds ($\text{FC}(\text{C}-\text{C})$; upper ---; ●; $r^2 = 0.978$); 3) $^1\text{FC}(\text{CC})$ values for formal C–C double bonds ($\text{FC}(\text{C}=\text{C})$; lower ---; ●; $r^2 = 0.958$); 4) all $^1\text{FC}[\sigma(\text{CC})]$ values (upper —; ◇; $r^2 = 0.776$); 5) $^1\text{FC}[\sigma(\text{CC})]$ values just for formal C–C single bonds ($^1\text{FC}[\sigma(\text{C}-\text{C})]$; upper ---; ◇; $r^2 = 0.996$); 6) $^1\text{FC}[\sigma(\text{CC})]$ values just for C–C double bonds ($^1\text{FC}[\sigma(\text{C}=\text{C})]$; lower ---; ◇; $r^2 = 0.947$). CP-DFT/B3LYP[7s,6p,2d/4s,2p] calculations.

with the s character of the C–C bond: The perfect linear relationship between the FC term and its orbital contributions is with the spin densities at the perturbed and responding nuclei according to Equation (10). There is no general relationship between the FC term and bond properties such as s -character, bond length, bond stretching frequency, etc., which accurately describes the nature of the CC bond. There are, however, useful relationships for well-defined classes of CC bonds. The FC term,

and in particular its contributions, is much more sensitive to changes in the electronic environment of a bond than to changes in the bond length (compare single bonds in methylacetylene and *trans*-1,3-butadiene: $R = 1.46 \text{ \AA}$ in both cases, $\omega_a = 1216$ and 1207 cm^{-1} , but the FC values of 73 and 55 Hz differ by 18 Hz; Tables 3 and 4).

4.3. NC Contributions

In Table 3, PSO and SD terms, as well as their different orbital contributions, are listed for the CC bonds considered. The SD term is always positive, whereas the PSO term can adopt both positive and negative values. As discussed in Section 2, the PSO term is close to zero for an isolated CC single bond, as in ethane. There is a small negative $\sigma(\text{CC})$ contribution of 0.7 Hz, which is canceled by a positive contribution $\sigma(\text{CH}) = 0.65 \text{ Hz}$. As soon as the formal C–C single bond adopts some π character by hyperconjugation (see, for example, propene) or by π conjugation (see, for example, butadiene), the PSO term becomes negative (-1.3 and -3 Hz , respectively; Table 3). For real π bonds, PSO values between -7.2 Hz (benzene) and -10.3 Hz (ethene, Table 3) were found. An increase in the multiple bond character reduced the PSO term (see allene: -7.9 Hz) and finally led to a positive value of 8 Hz in the case of acetylene. Plotting the calculated PSO values as a function of the p character $\bar{p}(\text{CC})$ (see inset of Figure 5) led to a cubic dependence with a large scattering of points and a correlation coefficient r^2 of just 0.910. There are three groups of data points (single, double, and triple bonds) as well as some separated single points (single bond of methylacetylene, benzene, and allene).

The PSO terms dominate the NC terms Δ . In this way, the dependence of Δ on the p character \bar{p} of the C–C bond also adopted a cubic (Figure 5) rather than quadratic form, as was the case for the NC terms based on experimental data (Figure 1). If just the six molecules that are the basis for the quadratic relationship of Figure 1 are considered, the latter was reproduced with somewhat different coefficients and a slightly better correlation coefficient ($r^2 = 0.986$). Hence, the difference between the correlations in Figures 1 and 5 results from the fact that the number of measured SSCCs available for investigating the dependence of Δ on the p character \bar{p} is too small to provide a reliable description. This is given by the calculated data displayed in Figure 5.

Figure 5 reveals that there is a similar clustering and scattering of Δ points ($r^2 = 0.953$) as found for the PSO term. The SD term correlates somewhat better with \bar{p} ($r^2 = 0.986$, Figure 5) because the SD term is always positive and increases steadily with increasing p character \bar{p} . Clearly, theory reveals that there is just a qualitative relationship between NC terms and p character. Since this could indicate that \bar{p} is not a suitable parameter for assessing the magnitude of the NC terms, we have investigated its relationship to other bond properties.

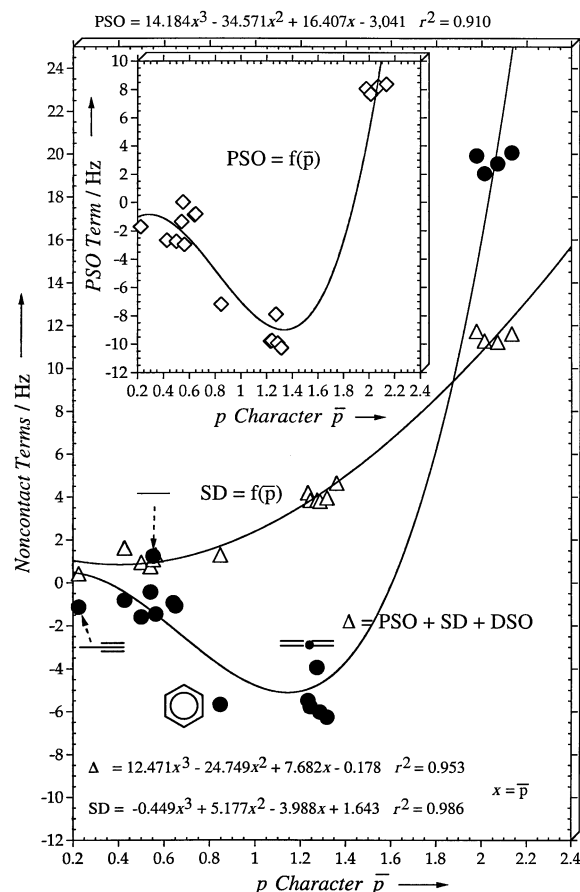


Figure 5. Functional dependence of the calculated $^1\text{NC}(\text{CC})$ part Δ (●), the $^1\text{SD}(\text{CC})$ term (Δ), and the $^1\text{PSO}(\text{CC})$ term (\diamond ; inset) on the total p-character \bar{p} of a C–C bond according to calculated SSCCs. CP-DFT/B3LYP[7s,6p,2d/4s,2p] calculations.

In Figure 6, bond order AOM, NRT, and the p character \bar{p} are compared. Both the AOM and the NRT bond order underestimate bond conjugation in 1,3-butadiene, vinylacetylene, and in 1,3-butadiene, as becomes obvious when comparing bond

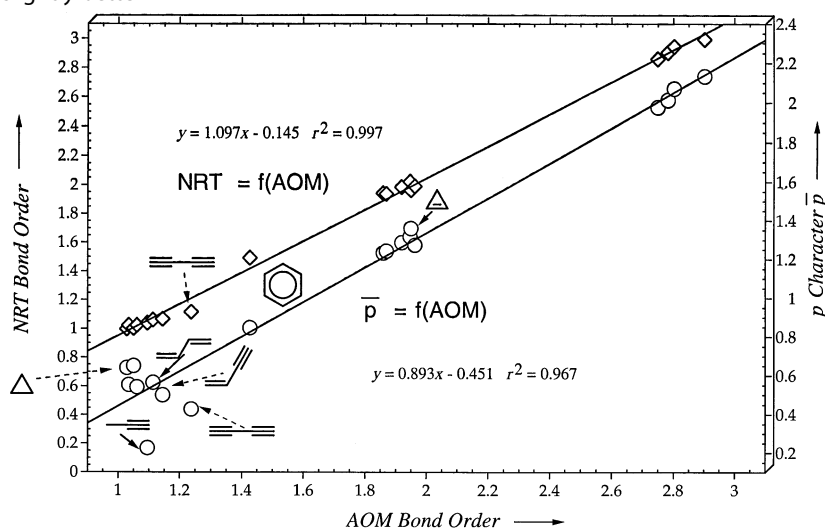


Figure 6. Comparison of the p character $\bar{p}(\text{CC})$ and the bond order NRT(CC) with the bond order AOM(CC). B3LYP6-31G(d,p) calculations.

orders with bond lengths and bond-stretching frequencies. In these cases, the AOM bond order provides a somewhat better description, and therefore this bond order has been used as the reference (Figure 6) for evaluating the usefulness of \bar{p} .

Clearly, \bar{p} correlates only in limited way with the bond order AOM. C–C single bonds involving sp -hybridized carbon atoms have a much lower p character than single bonds between sp^3 -hybridized carbon atoms. Since this is not compensated by the π bond order caused by π conjugation, the p character of the single bond in 1,3-butadiyne or vinylacetylene becomes much smaller than that of the single bond in propene or ethane. We will see in the following that this causes the actual problem of correlating the PSO terms with \bar{p} .

Since the AOM bond order provides a parameter better suited to identifying different types of C–C bonding, calculated NC terms are correlated with this bond order in Figures 7a and 7b. Indeed, the cubic relationship between Δ , PSO, and the SD term and the AOM bond order are improved so that the scattering of data points is significantly less (SD: $r^2 = 0.990$; PSO: $r^2 = 0.971$; Δ : $r^2 = 0.977$) than in the case of the correlation with \bar{p} (Figure 5). Despite these improvements, the NC term Δ can hardly be used for a quantitative description of C–C bonds. There is the possibility of distinguishing C–C single, double, and triple bonds because they lead to clearly different NC values. Also, aromatic and allenic C–C bonds can be distinguished (Figure 7b). However, a differentiation of conjugated C–C bonds (either single, double, or triple) is hardly possible. This results from the clustering of PSO values when correlated with the AOM bond order. However, even the SD term, which correlates much better with the AOM values, reveals some clustering of the data points (Figure 7a). When the NC values are compared with bond lengths $R(\text{CC})$ and adiabatic stretching frequencies $\omega_a(\text{CC})$ (not shown), then a basic problem emerges. The π character—and by this the bond strength of the conjugated formal single bonds (1,3-butadiyne, vinylacetylene, 1,3-butadiene)—is clearly underestimated by the NC terms: This happens to be a deficiency of the NRT and AOM bond orders also. For AOM bond orders decreasing towards zero, both the PSO, the SD, and the NC term must approach zero. If this condition is imposed on the correlation curves in Figure 7, even the scattering of data points for bond orders close to 1 is enhanced. In the following, we will explain these deficiencies by an analysis of the PSO term.

The PSO operator is an angular momentum operator, which leads to three different contributions of the type xy , xz , and yz . The magnitude of the PSO interactions becomes large in the presence of high-lying occupied and low-lying virtual orbitals with significant p character at the coupling nuclei. Hence, excitations $p\sigma(\text{CC}) \rightarrow p\pi^*(\text{CC})$, $p\pi(\text{CC}) \rightarrow p\sigma^*(\text{CC})$, $p\pi_x(\text{CC}) \rightarrow p\pi_y^*(\text{CC})$, etc. play an important role. These can be complemented by excitations $p\sigma(\text{CH}) \rightarrow p\pi^*(\text{CC})$, etc., provided that the C–H bond is polar, thus causing an anisotropic density distribution at the hydrogen atom (leading to the inclusion of a p -type polarization function at the H atom to describe the C–H orbitals). This is the case when the increasing electronegativity of sp^2 - and sp -hybridized carbon atoms leads to a polar C–H bond. The s orbitals do not contribute to the PSO term, which accordingly cannot probe the density at the coupling nuclei.

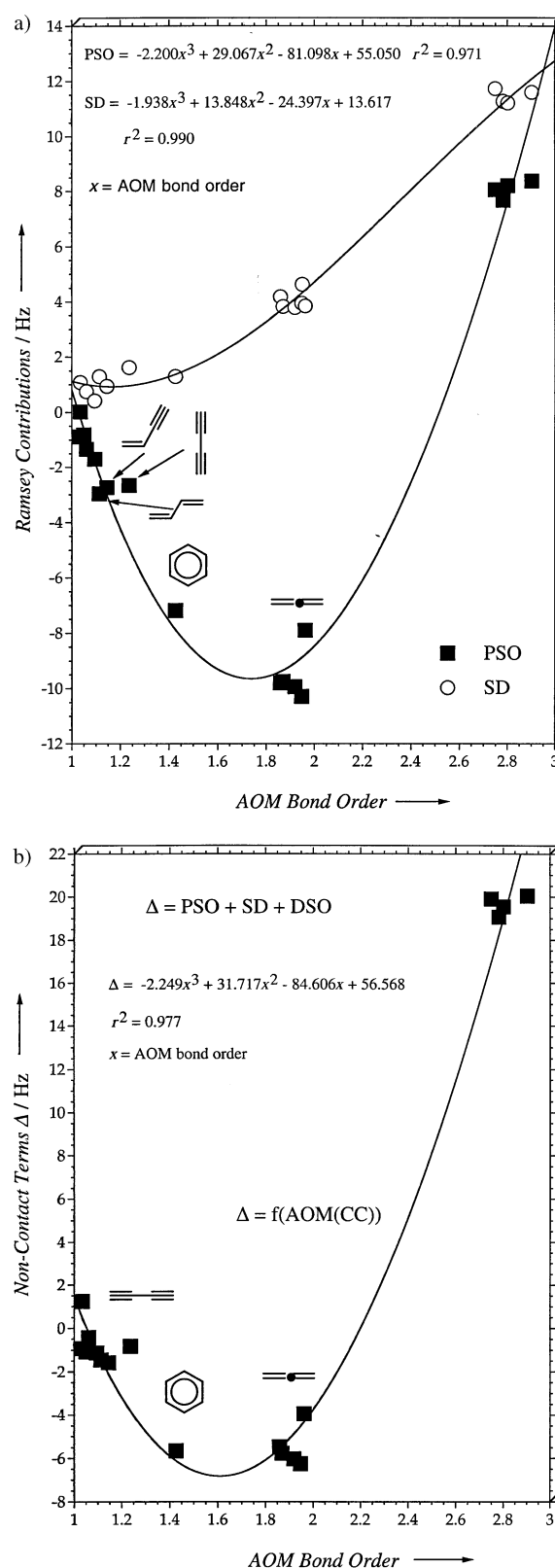


Figure 7. Functional dependence of a) the calculated noncontact terms ${}^1\text{SD}(\text{CC})$ (\circ) and ${}^1\text{PSO}(\text{CC})$ (\blacksquare); b) the ${}^1\text{NC}(\text{CC})$ sum, Δ , (\blacksquare) on the bond order AOM(CC). All SSCC terms calculated at the CP-DFT/B3LYP[7s,6p,2d/4s,2p] level of theory.

Both the DSO and PSO terms describe the coupling between the nuclei mediated by orbital currents in the molecule. The perturbing nucleus induces these currents, which in turn gives rise to an extra magnetic field. The value and orientation of this field at the responding nucleus favors either a parallel or an antiparallel orientation of the magnetic moments of the perturbing and responding nuclei. For a given orientation of the perturbing nucleus, the DSO and PSO terms can be written as a weighted integral over the electronic current density, where the weighting factor extracts that part of the total current density that forms a ring current around the responding nucleus. The isotropic PSO term considered in this work is then the average over the three contributions PSO_x , PSO_y , and PSO_z , where each of these three terms is dominated by one or more orbital contributions.

Even when the dominating contributions in terms of electron excitations are identified and analyzed, weighting and averaging to obtain the isotropic PSO term can lead to unforeseen results. Since a detailed analysis is given elsewhere,^[39] here the most important results are summarized. Terms involving $p\sigma \rightarrow p\pi^*$ or $p\pi \rightarrow p\sigma^*$ excitations lead to negative, and terms involving $p\pi_x \rightarrow p\pi_y^*$, etc. excitations lead to positive, PSO contributions. The π part of the triple bond values is quite large (18 Hz), however due to different signs of the PSO terms resulting from electron currents around the bond axis (positive; $p\pi_x \rightarrow p\pi_y^*$) and from those around axes perpendicular to the bond axis (negative; excitations involving either $p\sigma$ or $p\sigma^*$), the triple bond values are just at about 8 Hz. This is confirmed by Figure 8, in which the $\sigma(\text{CC})$ and $\pi(\text{CC})$ orbital contributions of $^1\text{PSO}(\text{CC})$ are plotted against the AOM bond order. Hence, the parabolic- or cubic-type curves found for $\Delta(\text{CC})$ (Figure 7b) and $\text{PSO}(\text{CC})$ (Figure 7a) are both a result of the $^1\text{PSO}[\pi(\text{CC})]$ contribution. The contribution $^1\text{PSO}[\sigma(\text{CC})]$ changes regularly with the AOM bond order ($r^2 = 0.992$, Figure 8) and is negative throughout, thus increasing the difference in the PSO term for CC double and

triple bonds. In other words, for the CC double bond, both PSO_x , PSO_y , and PSO_z are negative, thus leading to a larger (negative) magnitude than in the case of the C–C triple bond where $\sigma(\text{CC})$ and $\pi(\text{CC})$ orbital contributions partially cancel each other.

Since the clustering of the PSO points arises from the $\pi(\text{CC})$ orbital contribution, the reason the PSO term—and by this the NC term $\Delta(\text{CC})$ —is less suitable for a detailed analysis of C–C bonds of the same type (single, double or triple) can be clarified. In the case of the single bonds in conjugated π systems, orbital currents around the bond axis have different directions at the perturbing and responding nuclei, thus leading to more positive $^1\text{PSO}[\pi(\text{CC})]$ contributions than expected from bond lengths or adiabatic stretching frequencies.

The changes in the SD term (Figure 7a) are smaller than those in the PSO term. It increases from 1 Hz (ethane) to 3.9 Hz (ethene) and 11.6 Hz (acetylene) where the changes are dominated by the positive $\pi(\text{CC})$ orbital contribution, which is often somewhat larger than the total SD term. For the SD mechanism to be effective, a pair of an occupied $p\pi$ and a low-lying unoccupied $p\pi^*$ orbitals is necessary, which becomes obvious when considering the form of the SD operator.^[28] The triple bond, which has two sets of $\pi-\pi^*$ -orbitals, is characterized by a much larger $\text{SD}[\pi(\text{CC})]$ orbital contribution (13.4 Hz) than the double bond in ethene (5.3 Hz), or the formal single bond C2C3 in butadiene (1 Hz, Table 3). Hence, the $\pi-\pi^*$ pairs for C–C bonds with π character are important for an effective SD interaction, as well as for an effective PSO interaction mechanism. They can be used with different success to assess the π character of a C–C bond.

5. Chemical Relevance of the Results, and Conclusions

The NC terms PSO and SD provide different measures of the p electrons participating in C–C bonding. The SD term reflects the degree of π bonding where both pure π bonds, but also hyperconjugative interactions with pseudo- π orbitals lead to SD contributions. The PSO term is also sensitive to the $p\sigma$ orbitals and therefore should be compared with a property that includes all p electrons. If one takes the sum of these two terms, a satisfactory correlation with the π character of a C–C bond cannot be expected. A semiquantitative measure for the magnitude of the NC terms is provided by the p character, \bar{p} , of a bond, which can be used to describe a C–C bond provided a way is found to separate the FC term from the total SSCC. This will work to a certain extent in the case of hydrocarbons, if C–C and C–H bonding in these molecules is described with the help of hybrid orbitals and both $^1J(\text{CC})$ and all one-bond SSCC for the substituent bonds are known. Utilizing Equations (4), (5), and (6), the p-character of the C–C bonds—or better, the AOM bond order—can be assessed using both measured $^1J(\text{CH})$ and $^1J(\text{CC})$ values. Hence, a semiquantitative description of \bar{p} can be given with

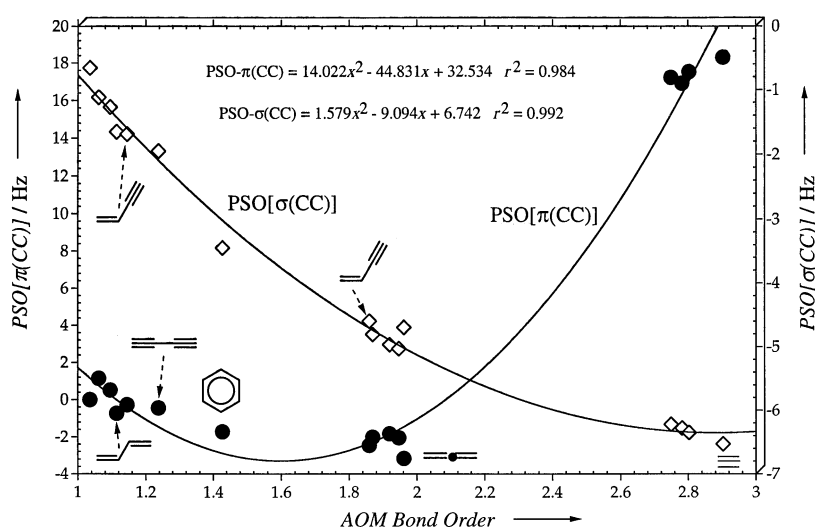


Figure 8. Functional dependence of the calculated orbital contributions $^1\text{PSO}[\sigma(\text{CC})]$ (\diamond) and $^1\text{PSO}[\pi(\text{CC})]$ (filled circles) on the bond order AOM(CC). All SSCC terms calculated at the CP-DFT/B3LYP[7s,6p,2d/4s,2p] level of theory.

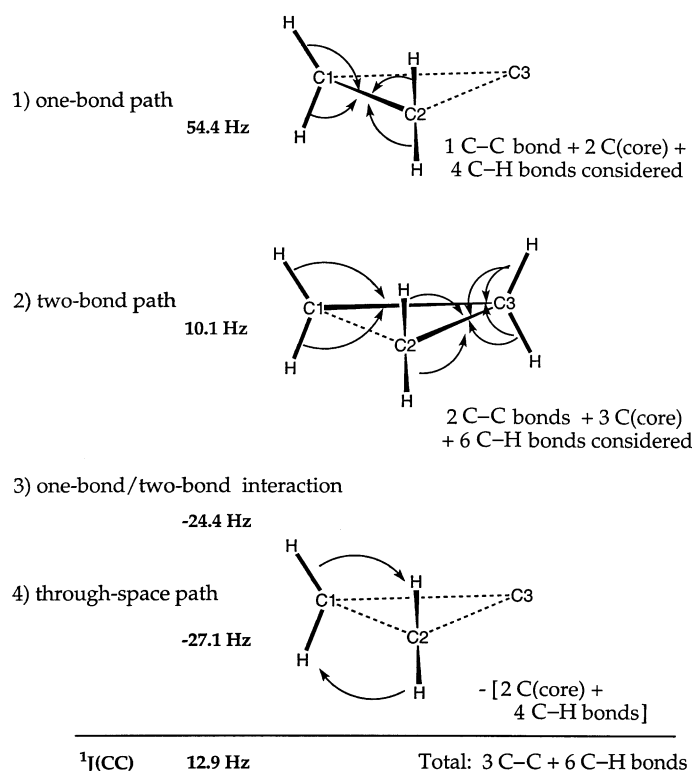
the help of the SSCCs, out of which the π character (AOM bond order) of the C–C bond can be extracted. For the purpose of testing the ability of this approach, in the following we investigate cyclopropane and cyclopropene. These strained ring systems are known to possess C–C bonds with increased p character.^[49] The Walsh orbitals of cyclopropane are formed by p orbitals, which lead to the bent bonds of the three-membered ring.^[49] We will see whether the method described above can lead to a useful description of C–C bonding in strained rings.

5.1. Determining the p Character of a Strained Bond

The measured $^1J(\text{CC})$ value of cyclopropane is just 12.4 Hz,^[19] which is significantly smaller than that of typical C–C single bonds (about 35 Hz, Table 3). For cycloalkanes, however, this value decreases stepwise with decreasing ring size: 32.7 Hz for cyclohexane, 31.1 Hz for cyclopentane, 27.8 Hz for cyclobutane, and, finally, just 12.4 Hz for cyclopropane.^[19] The reason for this decrease is closely connected to an increased importance of multi-path coupling.^[25]

The *J*-OC-PSP calculations reveal that the C–C one-bond path contributes in total 54.4 Hz (see Scheme 3), which is between the $^1J(\text{CC})$ of ethane (34.6 Hz) and the $^1J(\text{CC})$ of ethene (67.6 Hz, Table 3). The two-bond path adds another 10.1 Hz, typical of a geminal CC coupling in strained rings,^[19] but with opposite sign. There is also a through-space path of the SSCC, which adds –27.1 Hz to the $^1J(\text{CC})$ of cyclopropane, indicating that the interactions between the back-lobes of the CH hybrid orbitals through-space play an important role. The sum of these contributions (10.1 – 27.1 = –17 Hz) leads to a strongly negative contribution, as one would expect for a ring with high strain. There is also a strong interaction between the orbitals constituting the one-bond and the two-bond path, which leads to a path–path interaction and a contribution of –24.5 Hz, thus reducing the large one-bond path contribution to the relatively small total SSCC of 12.9 Hz (measured 12.4 Hz^[19]). Hence it would be highly misleading to describe the character of the C–C bond in cyclopropane on the basis of the measured $^1J(\text{CC})$ value.

On the other hand, the calculated NC value for $^1J(\text{CC})$ of cyclopropane is –0.85 Hz (Scheme 3) and seems to indicate an increased p character of the C–C bond. Extending the investigation to cyclopropene (Scheme 3) leads to values of –1.08 and –1.37 Hz, respectively for the NC terms (total values 8.6 and 66.0 Hz, Scheme 3) of $^1J(\text{C–C})$ and $^1J(\text{C=C})$. The single-bond value is in line with the cyclopropane value, whereas the double-bond value is more positive than the ethene value of –6.3 Hz (Table 3). This could indicate that the double bond in cyclopropene already has partial triple bond character. However, there are reasons to reject this assumption: The calculated value of \bar{p} obtained with different methods and basis sets is always smaller than 1.5, suggesting a similar value of \bar{p} to that found in allene. The NC term of allene is, however, –3.94, which means that a NC term of –1.37 Hz must correspond to a bond with



Scheme 3. Explanation of different path contributions to the SSCC $^1J(\text{CC})$ in cyclopropane. The bonds contributing to a particular path are given in bold. The path contribution in Hz is also given in bold (CP-DFT/B3LYP[7s,6p,2d/4s,2p] calculations; analysis with the *J*-OC-PSP method; see text.) The calculated $^1J(\text{CC})$ and the corresponding Ramsey values for cyclopropane and cyclopropene are also given.

significantly more π -character than the allene double bond possesses. Hence, the NC term and p character contradict each other, suggesting that because of multipath coupling a reasonable analysis cannot be carried out.

When attempting to estimate the p character of an unknown C–C bond using the quadratic function, Equation (7), the environment of the C–C bond has to be considered. Application to strained ring systems does not lead to any reasonable result because of multipath coupling. However, an assessment of the p character of unusual C–C bonds of acyclic and unstrained cyclic molecules (carbocations with and without charge delocalization, C–C bonds elongated by strong steric repulsion, homoaromatic C–C bonds, C–C bonds in metallocenes and other transition-metal complexes, etc.) should be possible, provided there is sufficient information on the bonds attached to the C–C bond under investigation. We suggest that the actual description of such a bond is supported by SSCC calculations and an orbital decomposition using *J*-OC-PSP.

This work has provided an insight into the spin–spin coupling mechanism, leading to the one-bond SSCC $^1J(\text{CC})$ in hydro-

carbons with single, multiple, and strained bonds. The following conclusions can be drawn:

- 1) The one bond SSCC $^1J(\text{CC})$ was tested as a possible descriptor for the nature of the CC bond. Since the SSCC probes different properties of the electron density distribution at the same time, it can only be used for a description of the bond if it is possible to decode the various mechanisms leading to spin–spin coupling. Separating the FC and NC terms is a possible way of achieving this, and leads to a useful, semiquantitative description of CC bonding, complementing that obtained by other bond properties.
- 2) The FC term correlates linearly with the spin density distribution at the coupling nuclei according to Equation (10). *The often used s density at the coupling nuclei or the s character of the LMOs forming the bond are not reliable measures of the FC(CC) term.* As a matter of fact, there exists no satisfactory relationship between FC(CC) and the s character $s_{\text{A}}s_{\text{B}}$ of the type shown in Equation (4). Such a relationship seems to be only fulfilled for the different types of C–C single bonds, but not necessarily for C–C double or C–C triple bonds. This limits the possibility of separating the FC and the NC term in a quantitative way.
- 3) The $^1\text{FC}(\text{CC})$ term is dominated by the orbital contribution $\sigma(\text{CC})$, which behaves differently for C–C single, double, and triple bonds (Figure 4a). The orbital contributions of substituent bonds add negative values to the FC term and by this lead to a larger scattering in the $^1\text{FC}(\text{CC})$ data points. This means that $^1\text{FC}(\text{CC})$ is first of all a local, rather than a bond, property; second it depends on the first order density (the spin density) rather than the s density; and, finally, it is influenced by all bonds attached to the C–C bond under consideration. The difference between the (zeroth-order) s density (or the s character) and the s spin density at the coupling nuclei can be assessed by considering that the first depends on the electronegativity (depending in turn on the topology of bonding and the degree of hybridization), the latter on the polarizability of the carbon atoms involved in spin–spin coupling.
- 4) The importance of the NC terms increases with increasing multiple bond character. It decreases from 1.2 Hz (normal C–C single bond), to -0.4 (C–C single bond with hyperconjugation), -1.5 (formal C–C single bond in a conjugated system), -5.7 (aromatic bond), and -6 Hz (double bond), and then it increases again to -3.9 (allene double bond), and 20 Hz (C–C triple bonds). The cubic-type dependence of the NC term on the p character or the bond order results from the PSO term, which in turn adopts this form from the orbital contribution $\pi(\text{CC})$.
- 5) The orbital contribution $^1\text{PSO}[\pi(\text{CC})]$ primarily reflects the changes in the orbital currents around the bond axis and around axes perpendicular to the bond. The latter are always present and lead to negative PSO contributions, whereas the former are found for bonds with either π_x and π_y orbitals or x,y combinations of π and pseudo- π orbitals, which yield positive values. The positive contributions can outweigh the negative contributions only for C–C triple bonds, thus these are the only C–C bonds with a relatively large positive $^1\text{PSO}[\pi(\text{CC})]$ and $^1\text{PSO}(\text{CC})$ term, leading to a relatively large NC term. The PSO term clearly distinguishes between C–C triple bonds (8 Hz), C–C double bonds (-10 Hz), aromatic C–C bonds (-7 Hz), and C–C single bonds (-3 to 0 Hz).
- 6) The PSO term probes the perturbation of orbital currents, which relates to the ease of exciting electrons from occupied to unoccupied orbitals. Orbital currents can enhance or diminish each other. This depends on the presence of certain types of electrons, which of course is also of importance for the strength of the chemical bond. However, the PSO term is the sum of several different orbital currents, each weighted and averaged so that its relationship to other bond properties, such as bond length, bond order, etc., is given in a semiquantitative, rather than quantitative, manner.
- 7) The SD(CC) term results primarily from the (positive) one-orbital π contributions, which arise from $\pi \rightarrow \pi^*$ excitations. Small contributions (either positive or negative) are also given by pseudo- π orbitals. The positive SD terms increase cubically (or exponentially) with the AOM bond order and p character of the C–C bond ($r^2 = 0.990$ and 0.986). One could argue that the SD term is best suited to describing the multiple character of a C–C bond, however, a differentiation between different C–C double bonds or triple bonds is not possible with the SD term.
- 8) It has been shown in this work that it is not possible to use the NC terms of $^1J(\text{CC})$ to describe C–C bonding in small, strained rings. In these ring systems, multipath coupling complicates the spin–spin coupling mechanism. Calculated data points for cyclopropane and cyclopropene do not fulfill the relationships found for the acyclic hydrocarbons.
- 9) In general, the p character, \bar{p} , is not a useful parameter for describing either the C–C bonding characteristics or the NC term Δ . Since it requires the addition of the p character of a hybrid orbital and the π character m , Equation (6), different measures for p electron interactions are mixed, which leads to contradictory answers concerning formal single bonds in conjugated systems. For example, the single bond in 1,3-butadiene has a smaller p character than the single bond in ethane. Similar deficiencies were found when describing vinylacetylene or 1,3-butadiene. The result obtained for the experimental $^1J(\text{CC})$ data (Figure 1) is misleading because the number of data points is too small to be representative.
- 10) It is noteworthy that all bond orders tested in this work underestimate the effect of π conjugation on formal C–C single bonds. This becomes obvious when correlating bond lengths $R(\text{CC})$ or adiabatic stretching frequencies $\omega_{\text{a}}(\text{CC})$ with \bar{p} or the AOM and NRT bond orders. This could be a consequence of the fact that, for these parameters, LMOs are used to describe the C–C bond. In general, π conjugation is better described by canonical MOs.
- 11) There is a need to reconsider—with the help of quantum chemical calculations—empirical relationships such as Equations (4) and (6), which relate SSCC J to the s character of the hybrid orbitals forming the bond. Even if a method such as CP-DFT does not provide exact SSCCs, and even if vibrational corrections for J cannot be calculated for large molecules, a linear relationship between calculated and measured

SSCCs—as is shown in Figure 2—will provide a reliable basis for testing the dependence of the SSCC on other bond parameters. A simple test in this respect is to investigate the relationship between s density and s spin density at the coupling nuclei.

- 12) There is clearly no basis for the correlation of SSCCs $^1J(CC)$ with bond properties, such as bond length, bond-stretching frequencies, etc. Previous attempts in this direction were misleading because the number of data points was too small. Nevertheless, the relationships between the NC term of the SSCC $^1J(CC)$ and the AOM bond order helps to identify the multiple bond character of a C–C bond and can be used in this way.

The SSCC is a sensitive measure for different properties of the bond density and the total bonding environment, including substituent bonds as well as proximal molecular parts, which may act through-space (not investigated in this work). The information contained in the SSCC is difficult to decode and therefore new methods and tools, such as $J\text{-OC-PSP}$, the FC spin density distribution, the orbital current density, and the PSO density distribution^[15, 35, 36, 39] are needed in order to unravel the spin–spin coupling mechanism and its dependence on the electronic structure of a molecule. In future, the successful interpretation of SSCCs $^1J(CC)$ will require a combination of measurements and quantum chemical calculations.

Acknowledgements

This work was supported by the Swedish Research Council (Vetenskapsrådet). Calculations were done on the supercomputers of the Nationellt Superdatorcentrum (NSC), Linköping, Sweden. D.C. and E.K. thank the NSC for a generous allotment of computer time.

Keywords: carbon–carbon bonds • coupling constants • Fermi contacts • NMR spectroscopy

- [1] L. Pauling, *The nature of the chemical bond*, 3rd ed., Cornell University Press Ithaca, New York, 1960.
- [2] a) *Theoretical Models of Chemical Bonding, Part 2, The Concept of the Chemical Bond* (Ed.: Z. B. Maksic), Springer Verlag, Heidelberg, 1990; b) R. McWeeny, *Coulsons Chemische Bindung*, Hirzel, Stuttgart, 1984; c) R. T. Sanderson, *Chemical Bonds and Bond Energy*, Academic Press, New York, 1976.
- [3] B. M. Gimarc, *Molecular structure and bonding—the qualitative molecular orbital approach*, Academic Press, New York, 1979.
- [4] P. Coppens, M. B. Hall, *Electron density distributions and the chemical bond*, Plenum Press, New York, 1981.
- [5] a) K. Ruedenberg, in *Localization and delocalization in quantum chemistry* (Eds.: O. Chelvet, R. Daudel, S. Diner, J. P. Malrien), D. Reidel Publishing Co, Dordrecht, (Vol. I), 1975, p. 223; b) K. Ruedenberg, *Rev. Mod. Phys.* 1962, 34, 326.
- [6] a) W. Kutzelnigg, *Angew. Chem.* 1973, 85, 551; *Angew. Chem. Int. Ed. Engl.* 1973, 13, 546; b) F. Driessler, W. Kutzelnigg, *Theoret. Chim. Acta* 1976, 43, 1.
- [7] a) D. Cremer, E. Kraka, *Angew. Chem.* 1984, 96, 612; *Angew. Chem. Int. Ed. Engl.* 1984, 23, 627; b) D. Cremer, E. Kraka, *Croatica Chem. Acta*, 1984, 57, 1259.
- [8] E. Kraka, D. Cremer, in *Theoretical Models of Chemical Bonding, Part 2: The Concept of the Chemical Bond* (Ed.: Z. B. Maksic), Springer Verlag, Heidelberg, 1990, p. 453.
- [9] D. Cremer, A. Wu, A. J. Larsson, E. Kraka, *J. Mol. Modelling* 2000, 6, 396.
- [10] D. Cremer, A. J. Larsson, E. Kraka, in *Theoretical Organic Chemistry, Theoretical and Computational Chemistry*, Vol. 5, Elsevier, Amsterdam, 1998, p. 259.
- [11] J. A. Larsson, D. Cremer, *J. Mol. Struct.* 1999, 485, 385.
- [12] D. Cremer, E. Kraka, *J. Am. Chem. Soc.* 1985, 107, 3800.
- [13] N. Muller, D. E. Pritchard, *J. Chem. Phys.* 1959, 31, 768.
- [14] M. D. Newton, J. M. Schulman, M. M. Manus, *J. Am. Chem. Soc.* 1974, 96, 17.
- [15] R. M. Lynden-Bell, N. Sheppard, *Proc. Roy. Soc. A* 1962, 269, 385.
- [16] a) K. Frei, H. J. Bernstein, *J. Chem. Phys.* 1963, 38, 1216; b) H. Günther, W. Herrig, *Chem. Ber.* 1973, 106, 3938.
- [17] P. E. Hansen, *Org. Magn. Reson.* 1979, 12, 109.
- [18] W. A. Bingel, W. Lüttke, *Angew. Chem.* 1981, 93, 944; *Angew. Chem. Int. Ed. Engl.* 1981, 20, 899.
- [19] H. O. Kalinowski, S. Berger, S. Braun, *¹³C NMR-Spektroskopie*, Thieme, New York, 1984.
- [20] H. Günther, *NMR-Spektroskopie*, Thieme, New York, 1983.
- [21] K. Kamienska-Trela, *Spectrochimica Acta* 1980, 36A, 239.
- [22] J. Wardeiner, W. Lüttke, R. Bergholz, R. Machinek, R. *Angew. Chem.* 1982, 94, 873; *Angew. Chem. Int. Ed. Engl.* 1982, 21, 872.
- [23] a) S. Berger, S. Braun, H. O. Kalinowski, *NMR-Spektroskopie von Nichtmetalle*, Vol. 1, *Grundlagen ¹⁷O-, ³³S- und ¹²⁹Xe-NMR-Spektroskopie*, Thieme, New York, 1992; b) S. Berger, S. Braun, H. O. Kalinowski, *NMR-Spektroskopie von Nichtmetalle*, Vol. 2, *¹⁵N-NMR-Spektroskopie*, Thieme, New York, 1992; c) S. Berger, S. Braun, H. O. Kalinowski, *NMR-Spektroskopie von Nichtmetalle*, Vol. 3, *³¹P NMR-Spektroskopie*, Thieme, New York, 1993.
- [24] W. Lüttke, *Lecture Notes*, Göttingen, 2000.
- [25] A. Wu, J. Gräfenstein, D. Cremer, *J. Chem. Phys. A* 2003, 107, 7043.
- [26] N. F. Ramsey, *Phys. Rev.* 1953, 91, 303.
- [27] a) J. A. Pople, W. G. Schneider, H. J. Bernstein, *High-resolution Nuclear Magnetic Resonance*, McGraw-Hill, New York, 1959; b) J. W. Emsley, J. Feeney, L. H. Sutcliffe, *High resolution nuclear magnetic resonance spectroscopy*, Pergamon, Oxford, 1966, p. 690; c) *Encyclopedia of Nuclear Magnetic Resonance* (Eds.: D. M. Grant, R. K. Harris), Wiley, Chichester, UK, Vol. 1–8, 1996.
- [28] V. Sychrovsky, J. Gräfenstein, D. Cremer, *J. Chem. Phys.* 2000, 113, 3530.
- [29] a) A. D. Becke, *J. Chem. Phys.* 1993, 98, 5648; b) A. D. Becke, *Phys. Rev. A* 1988, 38, 3098; c) C. Lee, W. Yang, R. P. Parr, *Phys. Rev. B* 1988, 37, 785.
- [30] U. Fleischer, W. Kutzelnigg, H.-H. Limbach, G. L. Martin, M. L. Martin, M. Schindler, *Deuterium and Shift Calculation, NMR—Basic Principles and Progress*, Vol. 23, Springer, Heidelberg, 1990, p. 165.
- [31] a) *MOGADOC, Molecular Gasphase Documentation*, University Ulm, 1999; b) J. Vogt, *Struct. Chem.* 1992, 3, 147; c) J. Vogt, *J. Mol. Spectrosc.* 1992, 155, 413.
- [32] P. C. Hariharan, J. A. Pople, *Theoret. Chim. Acta* 1973, 28, 213.
- [33] a) J. P. Perdew, in *Electronic Structure of Solids '91* (Eds.: P. Ziesche, H. Eschrig), Akademie-Verlag Berlin, 1991, p. 11; b) J. P. Perdew, Y. Wang, *Phys. Rev. B* 1992, 45, 13244.
- [34] a) V. Polo, E. Kraka, D. Cremer, *Mol. Phys.* 2002, 100, 1771; b) V. Polo, E. Kraka, D. Cremer, *Theor. Chem. Acc.* 2002, 107, 291; c) V. Polo, J. Gräfenstein, E. Kraka, D. Cremer, *Chem. Phys. Lett.* 2002, 352, 469; d) V. Polo, J. Gräfenstein, E. Kraka, D. Cremer, *Theor. Chem. Acc.* 2003, 109, 22.
- [35] a) J. Gräfenstein, A. Wu, D. Cremer, *J. Phys. Chem A* 2003, 107, 7043; b) J. Gräfenstein, T. Tuttle, D. Cremer, unpublished results.
- [36] A. Wu, D. Cremer, *Phys. Chem. Chem. Phys.* 2003, 5, 4541.
- [37] a) J. E. Carpenter, F. Weinhold, *J. Mol. Struct. (Theochem)* 1988, 46, 41; b) A. E. Reed, R. B. Weinstock, F. Weinhold, *J. Chem. Phys.* 1985, 83, 735; c) A. E. Reed, L. A. Curtiss, F. Weinhold, *Chem. Rev.* 1988, 88, 899.
- [38] S. F. Boys, *Rev. Mod. Phys.* 1960, 32, 296.
- [39] a) J. Gräfenstein, D. Cremer, *Chem. Phys. Lett.* 2004, 383, 332; b) J. Gräfenstein, D. Cremer, *Chem. Phys. Lett.*, in press.
- [40] E. Kraka, J. Gräfenstein, M. Filatov, Y. He, J. Gauss, A. Wu, V. Polo, L. Olsson, Z. Konkoli, Z. He, D. Cremer, *COLOGNE2003*, Göteborg University, Göteborg, 2003.
- [41] A. T. Ruden, O. B. Lutnas, T. Helgaker, K. Ruud, *J. Chem. Phys.* 2003, 118, 9572. In the case of acetylene, a vibrational correction of –10.0 Hz has to be added to the calculated $^1J(CC)$ value.

- [42] a) E. D. Glendening, F. Weinhold, *J. Comp. Chem.* **1998**, *19*, 593; b) E. D. Glendening, F. Weinhold, *J. Comp. Chem.* **1998**, *19*, 610; c) E. D. Glendening, J. K. Badenhoop, F. Weinhold, *J. Comp. Chem.* **1998**, *19*, 628.
- [43] J. Cioslowski, S. T. Mixon, *J. Am. Chem. Soc.* **1991**, *113*, 4142.
- [44] F. R. W. Bader, *Atoms in Molecules, a Quantum Theory*, International Series of Monographs on Chemistry, Vol. 22, Clarendon Press, Oxford, **1995**.
- [45] a) Z. Konkoli, D. Cremer, *Int. J. Quant. Chem.* **1998**, *67*, 1; b) Z. Konkoli, D. Cremer, *Int. J. Quant. Chem.* **1998**, *67*, 29.
- [46] D. Cremer, L. A. Larsson, E. Kraka, *Theoretical Organic Chemistry, Theoretical and Computational Chemistry*, Vol. 5, Elsevier, Amsterdam, **1998**, p. 259.
- [47] J. A. Pople, J. W. McIver, N. S. Ostlund, *J. Chem. Phys.* **1968** *49*, 2960.
- [48] J. A. Pople, D. L. Beveridge, *Approximate molecular orbital theory*, McGraw Hill, New York, **1970**.
- [49] D. Cremer, E. Kraka, K. J. Szabo, in *The Chemistry of the Cyclopropyl Group*, Vol. 2 (Ed.: Z. Rappoport), Wiley, New York, **1995**, p. 43.

Received: September 26, 2003 [F 987]